

# FINAL PUBLISHABLE REPORT

Grant Agreement number 16ENG08  
 Project short name MICEV  
 Project full title Metrology for inductive charging of electric vehicles

Project start date and duration:		1 <sup>st</sup> September 2017, duration 42 months
Coordinator: Mauro Zucca, INRIM		Tel: +390113919827
Project website address: <a href="https://www.micev.eu/">https://www.micev.eu/</a>		E-mail: <a href="mailto:m.zucca@inrim.it">m.zucca@inrim.it</a>
Internal Funded Partners:	External Funded Partners:	Unfunded Partners:
1 INRIM, Italy	5 Aalto, Finland	13 SPEAG, Switzerland
2 NPL, United Kingdom	6 CIRCE, Spain	
3 PTB, Germany	7 CNRS, France	
4 RISE, Sweden	8 POLITO, Italy	
	9 TU Delft, Netherlands	
	10 TÜV-SÜD PS, Germany	
	11 UNICAS, Italy	
	12 UNISA, Italy	
RMG: -		

## TABLE OF CONTENTS

<b>1</b>	<b>OVERVIEW .....</b>	<b>3</b>
<b>2</b>	<b>NEED.....</b>	<b>3</b>
<b>3</b>	<b>OBJECTIVES.....</b>	<b>3</b>
<b>4</b>	<b>RESULTS.....</b>	<b>4</b>
<b>4.1</b>	<b>Objective 1: To develop and characterise a new measurement system for IPT stations .....</b>	<b>4</b>
4.1.1	The Power Measurement Unit (PwMU).....	4
4.1.2	The new calibration Facility at PTB .....	5
4.1.3	The calibration results and conclusions .....	8
<b>4.2</b>	<b>Objective 2: Methods to determine the efficiency of static IPT stations. ....</b>	<b>10</b>
4.2.1	Assessment of the Overall Efficiency in WPT Stations (WPTS) for Electric Vehicles .....	10
4.2.2	Modeling the efficiency of static wireless power transfer stations.....	13
4.2.3	Comparing computed and measured results, benchmarking, and conclusions.....	16
<b>4.3</b>	<b>Objective 3: Dynamic inductive power transfer .....</b>	<b>17</b>
4.3.1	Modeling Dynamic wireless power transfer and identification of relevant parameters .....	17
4.3.2	A measurement system special requirements .....	20
4.3.3	Additional considerations and conclusions.....	22
<b>4.4</b>	<b>Objective 4: Human exposure to magnetic fields .....</b>	<b>24</b>
4.4.1	The new calibration facility at NPL and its validation. ....	24
4.4.1.1	New Helmholtz Coil System.....	24
4.4.1.2	Calibration of the New Helmholtz Coil System and intercomparison .....	26
4.4.2	To develop measurement protocols for the assessment of the human exposure .....	27
<b>5</b>	<b>IMPACT .....</b>	<b>31</b>
<b>6</b>	<b>LIST OF PUBLICATIONS.....</b>	<b>33</b>

## 1 Overview

Inductive charging via inductive power transfer (IPT) is a wireless charging technology that will be used with electric vehicles (EVs) in the near future. IPT offers many advantages over traditionally fuelled and other currently available EVs, such as charging whilst in motion, smaller batteries, and high autonomy. Such advantages also support the reduction of carbon dioxide (CO<sub>2</sub>) and fossil fuel consumption. However, IPT is still a new technology and accurate measurements of electrical and magnetic quantities involved in IPT technology for the charging of EVs are limited. This project addressed this issue by developing metrological techniques for measuring IPT efficiency to ensure traceability of electric and magnetic measurements with sufficient accuracy for the demands of EV industry.

## 2 Need

Air pollution is one of the major environmental concerns in the urban environment. Advancements in IPT can facilitate and hasten the growth of the EV industry directly benefiting the environment in terms of reducing CO<sub>2</sub> emissions and other pollutants. However, IPT is a novel technology and, in certain areas, still under development. Therefore, investment in IPT technologies are needed in order to keep Europe at the forefront of associated research and industry.

IPT requires, among other things, accurate models and measurements that can clearly (i) identify how electromagnetic emissions are compatible with any human exposure and (ii) how to correctly bill the energy transferred on board EVs. However, accurate measurement of electrical and magnetic quantities involved in IPT technology currently represents a challenge. In fact, the signal amplitudes are often as large as those of the energy distribution systems, while the frequency bandwidth involved is much wider. As IPT technology is largely still under development, the corresponding required measurement capabilities have not been realised yet and given the types of application, these traceable measurements are needed before the industry can develop further. For example, the waveform characteristics of the electric quantities that supply the EV inductive charging systems are very specific and require dedicated measurement techniques. Such techniques must also include an adequate calibration of the transducers, especially regarding dynamic charging, where the supply of power to the vehicle involves a transient regime.

Reliable, accurate, traceable electric power, efficiency, and magnetic field (MF) measurements are needed for IPT applications. This is not only for manufacturers of EVs or hybrid EVs (including the automotive sector), but their suppliers, associated certification bodies and related electric companies. Such information is necessary for the strict international requirements for EV with respect to accuracy, safety and, in a near future, energy billing.

## 3 Objectives

The goal of this project was the development of high-accuracy calibration facilities for the traceability of electric and magnetic measurements with sufficient accuracy for the demands of EV industry. The specific objectives of the project were:

1. To develop and characterise a power measurement unit for static wireless power transfer for on-board measurement with a relative uncertainty in the direct current (DC) circuit of  $10^{-3}$ , the frequencies of the alternating current (AC) transmission being up to 100 kHz – 150 kHz and powers up to 200 kW.
2. To develop methods to determine the efficiency of a static wireless power transfer system with a relative uncertainty of  $10^{-3}$  and taking the relevant parameters, particularly airgap and misalignment between the coupled coils into account.
3. To define the requirements for a power measurement unit for dynamic wireless power transfer, identify the relevant parameters (e.g. traffic conditions, speed, vehicle dimensions, power converter state, coil configurations) and estimate their effect on the measurement of the power transferred to the vehicle and on the system efficiency.
4. To set up a system for traceable calibration of MF meters and gradiometers for 10 kHz to 150 kHz and up to 100  $\mu$ T and field gradients up to 100  $\mu$ T/m with both sinusoidal and non-sinusoidal waveforms. The target expanded uncertainty for the system is 5 %. To develop measurement protocols for the assessment of the human exposure to the electromagnetic fields generated by these technologies, in

static and dynamic conditions, taking the compliance with the limits indicated by the guidelines of the International Commission on Nonionizing Radiation Protection (ICNIRP) into account.

5. To facilitate the take up of the technology and measurement infrastructure developed in the project by the measurement supply chain and end users and to provide metrology input and pre-normative research to the evolution of relevant international standards

## 4 Results

### 4.1 Objective 1: To develop and characterise a new measurement system for IPT stations

The design and realisation of a new measurement system called Power Measurement Unit (PwMU) was completed during the project. This is a new and traceable measurement system devoted to the inductive charging of EVs. The PwMU is able to accurately measure the power absorbed from the batteries, that adsorbed from the electric grid, and the ratio between the two previous quantities (efficiency). Moreover, it is able to determine the magnetic flux density levels in the charging station and to record all the measured values and waveforms. The realisation was achieved at INRIM, with the support of PTB, CIRCE and POLITO with RISE contributing to the preliminary calibration. The PWMU is fully described in [1] and briefly described in 4.1.1.

Regarding electrical measurements, the PwMU was calibrated at PTB, where a new reference power standard was developed and realised, with appropriate AC and DC generators, analog-to-digital (ADC) and digital-to-analog (DAC) converters, current and voltage sensors and control software. PTB realised this system with INRIM contributing to the voltage measurement chain [2,3]. The facility is briefly described in 4.1.2.

#### 4.1.1 The Power Measurement Unit (PwMU)

The PwMU is constituted of three units plus numerous accessories and transducers:

- ✓ one unit designed to stay on the ground side and perform measurement of the power, voltage and current adsorbed, called "Grid Unit" (GU);
- ✓ one unit that can be embarked on board the vehicle, called "Board Unit" (BU);
- ✓ one unit that an operator can easily move in the charging station, around and inside vehicles, for magnetic measurements, called "Magnetic Unit" (MU).

In addition to the three (logical) units, the PwMU is accompanied by 2 laptops, sensors and transducers, which include connectors, shunts, cables and three GPS antennas, having a non-negligible importance.

In static measurements, which mainly concern this project, BU and GU can be stationed in the same place. For their housing two racks have been designed for the purpose, so that the two units can be stacked and moved on wheels. Fig. 1 shows the overall measurement system.

A specific constructive choice was made to improve reliability. In fact, the measurement system is designed for measurements at the charging stations. Field operations and measurement complexity require additional reliability verification. Thus, also to avoid doubts about the measurement, the presence of a second

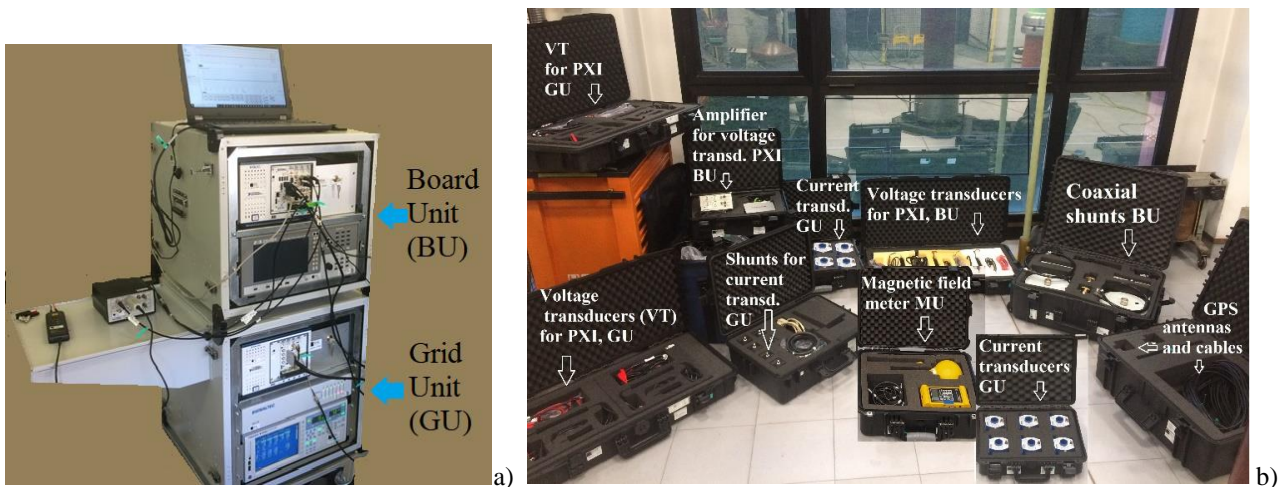


*Fig. 1 a) the two main modules of the PwMU, b) the main accessories of the PwMU*

measurement system may be useful. For this reason, GU and BU are equipped with a double measuring system.

The PwMU improves the ease and ability to characterise WPT (Wireless Power Transfer) charging stations both in field and in a laboratory environment.

#### 4.1.2 The new calibration Facility at PTB

A new calibration facility was developed in the framework of the MICEV project for three purposes: i) a specific calibration of the PwMU, ii) to study the effect of sinusoidal and non-sinusoidal voltage/current ripple on the measurement uncertainty concerning the power measurements on-board electric vehicles, and iii) to provide a new calibration service to industry.

To develop the facility, CIRCE, POLITO and RISE provided preliminary waveforms in order to start the facility design. The development of the facility has been done by PTB, with the collaboration of INRIM. The facility was completely developed at PTB in Braunschweig, Germany.

As regards the MICEV project, the interest is in the measurement of the active power transferred on board to the batteries, which, after removing any losses from the converters, provides the basis for the pricing. Battery voltage and current are DC signals with an AC ripple superimposed which, although limited, does not appear negligible.

For the development, construction and testing of the measuring system for combined AC and DC signals, two separate measuring systems for AC and DC were set up in a first step. Afterwards, they have been combined to measure mixed signals. The setup for the combined measurement is shown in the Fig. 2.

The required hardware components and their characteristics were determined and compared with those already available. Accordingly, some components were purchased, some built, or simply made available. The various components were then individually examined and characterised for their suitability.

Some of the components analysed and characterised are the following: digital to analog (D/A) converters, voltage amplifiers, transconductance amplifiers, voltage dividers, current shunts, analog to digital (A/D) converters. Among the investigations and effects analysed, we should mention the crosstalk of the current and voltage amplifiers and the crosstalk after amplifiers.

Correction was applied to converters. As an example, the remaining deviation of the A/D converters (ADC) after the correction, based on the characterisation of the ADC, is shown in Fig. 3.

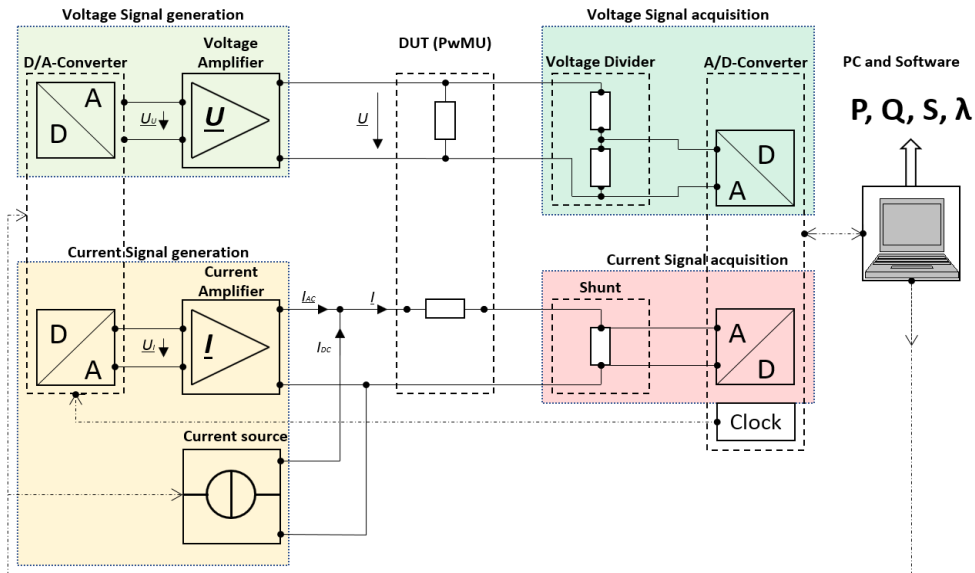


Fig. 2 Measurement setup for AC / DC signals

Based on the LabView development environment, programs for signal generation and signal recording adapted to the hardware components were created. This includes the generation of purely sinusoidal as well as non-sinusoidal signal characteristics. The control and readout of different test objects is also integrated.

To verify the extensive mathematical functions and the correct data flow, extensive tests were performed according to the black box principle. For this purpose, the synthetic waveforms generated in signal generation were fed directly back into the measuring program. This data is then treated in the measuring program exactly

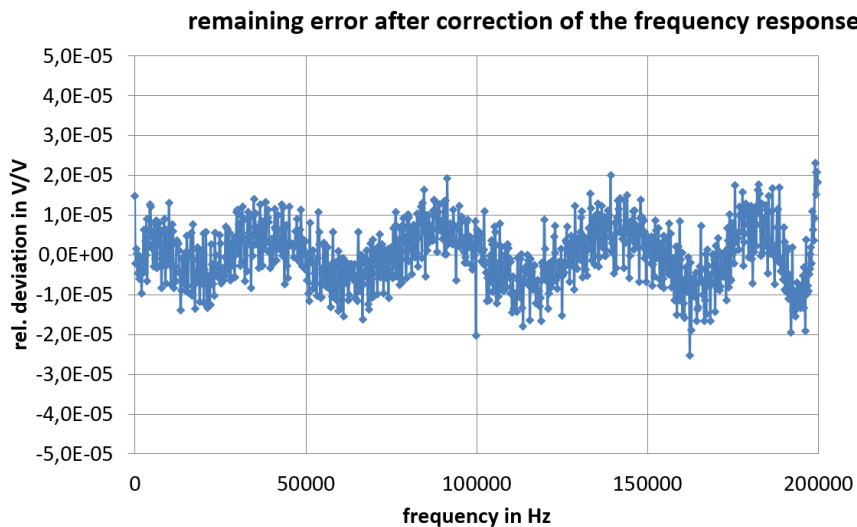


Fig. 3 Resulting frequency response of the A/D converter after correction

as if it had been recorded by the ADC. With the exact knowledge of the signal characteristics to be evaluated, a nominal value for the measurement result can be calculated and then compared with the actual value supplied by the measuring program. If no correction functions are active in the program, the result must correspond exactly to the target value.

As soon as correction functions are active, the output value of the measuring program is tuned in relation to the ideal set-point by the combination of the active correction functions. The resulting error is then subtracted from the desired correction. This difference represents the expected computational uncertainty of the software, which must be considered in the measurement uncertainty budget. This uncertainty arises, on the one hand, from the program limited numerical resolution and, to a large extent, from the simplification of the mathematical correction methods necessary for a prompt calculation of the measured values during the running measurement. An example of the amplitude correction of the voltage divider is shown in Fig. 4.

The various hardware components were sequentially combined step by step, until the complete measurement system was ready. This was done separately for AC and DC systems. The final measuring systems were then

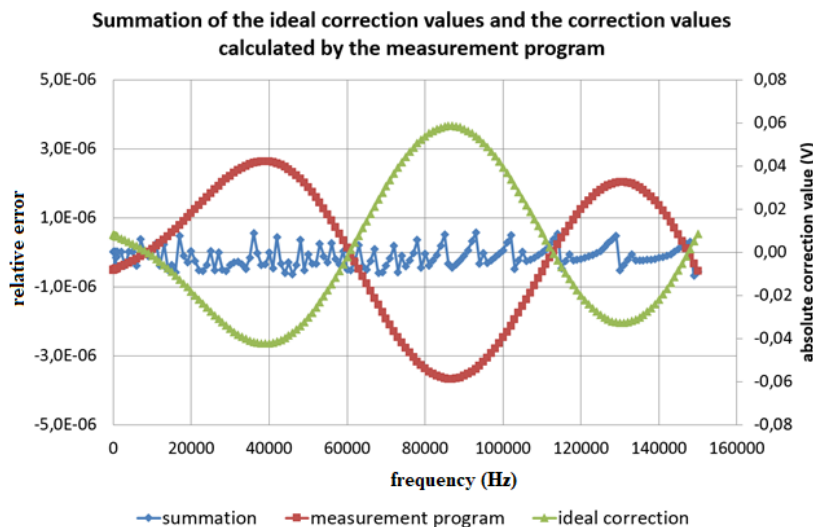


Fig. 4 Determination of the calculation error when correcting the amplitude of the voltage divider.

compared with low uncertainty measuring devices. Here, the measured deviations were compared with those expected from the hardware properties. Using the experience gained during the construction of the AC and DC reference systems, a measuring system for combined AC and DC signals was then completed and characterised.

The data derived from the characterisation of the individual hardware components, the measured value of the comparison measurements and the results of the software validation were transferred into individual uncertainty budgets. The values resulting from the AC and DC measurements were combined for the measurement system of the mixed quantities and the resulting additional influencing factors were extended. The measurement uncertainties resulting from the complex relationship between the different measured variables were summarised in tabular form for different value ranges. An excerpt of these measurement uncertainties is summarised in Tables I and II.

The measurements carried out at the charging stations showed a power factor of the AC component greater than 0.9. In two measurement campaigns at two different charging stations, an AC ripple power was measured that was always much lower than 0.1% of the DC power. The AC ripple has a predominant harmonic component at the double frequency with respect to the frequency of the resonant circuit. Then there are higher harmonics that make a negligible contribution to power. Table 2 allows the evaluation of the uncertainty also due to ripple in the DC measurement.

Table 1 Extract of the Table of the measurement uncertainties for AC

Measured variables	Power factor weighted average value of the AC components	Frequency weighted average value of the AC components (Hz)	$\delta S \frac{VA}{VA}$	$\delta P \frac{W}{VA}$	$\delta Q \frac{var}{VA}$
--------------------	--	--	--------------------------	-------------------------	---------------------------

$U = 30 \text{ V} - 240 \text{ V}$ $I = 0,1 \text{ A} - 14 \text{ A}$	$ \cos(\varphi)  = 1$	5-60	9,6E-05	9,6E-05	9,6E-05
	$ \cos(\varphi)  \geq 0,866$	5-60	9,6E-05	9,6E-05	9,6E-05
	$ \cos(\varphi)  \geq 0,5$	5-60	9,6E-05	9,6E-05	9,6E-05
	$ \cos(\varphi)  \geq 0$	5-60	9,6E-05	9,6E-05	9,6E-05
	$ \cos(\varphi)  = 1$	$\leq 150000$	5,0E-04	5,0E-04	7,1E-03
	$ \cos(\varphi)  \geq 0,866$	$\leq 150000$	5,0E-04	3,6E-03	6,2E-03
	$ \cos(\varphi)  \geq 0,5$	$\leq 150000$	5,0E-04	6,2E-03	4,6E-03
	$ \cos(\varphi)  \geq 0$	$\leq 150000$	5,0E-04	7,1E-03	5,0E-04

Table 2 Extract of the Table of the measurement uncertainties for DC+AC

Measured variables	Power factor weighted average value of the AC components	Frequency weighted average value of the AC components (Hz)	$\delta S \frac{VA}{VA}$	$\delta P \frac{W}{VA}$	$\delta Q \frac{var}{VA}$
$U_p = 30 \text{ V} - 1000 \text{ V}$ $I_p = 5 \text{ A} - 1000 \text{ A}$ Ratio AC/DC max 0.1 with $I_{ac \text{ peak max}} = 20 \text{ A}$	$ \cos(\varphi)  = 1$	5-60	1,4E-04	1,4E-04	1,4E-04
	$ \cos(\varphi)  \geq 0,866$	5-60	1,4E-04	1,4E-04	1,4E-04
	$ \cos(\varphi)  \geq 0,5$	5-60	1,4E-04	1,4E-04	1,4E-04
	$ \cos(\varphi)  \geq 0$	5-60	1,4E-04	1,4E-04	1,4E-04
	$ \cos(\varphi)  = 1$	$\leq 150000$	1,5E-04	1,5E-04	2,3E-03
	$ \cos(\varphi)  \geq 0,866$	$\leq 150000$	1,5E-04	1,1E-03	2,0E-03
	$ \cos(\varphi)  \geq 0,5$	$\leq 150000$	1,5E-04	2,0E-03	1,5E-03
	$ \cos(\varphi)  \geq 0$	$\leq 150000$	1,5E-04	2,3E-03	1,5E-04

#### 4.1.3 The calibration results and conclusions

In agreement with the project protocol, the BU of the PwMU was calibrated at PTB. The GU was calibrated in a facility for power frequency, while the BU was calibrated in the new calibration facility described in the previous section.

Several kinds of comparisons have been performed for the BU:

- Pure DC voltage and current;
- DC current and voltage overlapped to a sinusoidal AC signal (300 V<sub>DC</sub> + 100 V<sub>AC</sub>) and (500 V<sub>DC</sub> + 200 V<sub>AC</sub>) at the following frequencies: 25 kHz, 50 kHz, 75 kHz, 90 kHz, 110 kHz, 150 kHz;
- Current and voltage test signals as recorded in the transmission coil at a charging station;
- Current and voltage test signals as recorded in the receiving coil at a charging station;
- Current and voltage test signals as recorded at a charging station at the vehicle batteries.

The relative percentage difference between the measurement of the PTB facility and that of the PwMU was evaluated as:

$$\varepsilon = \frac{meas_{PTB} - meas_{PwMU}}{meas_{PTB}} \cdot 100 \quad (1)$$

and  $\varepsilon$  was always lower than 0.1%.

## Conclusions

Objective 1 was fully achieved with the implementation of the new PwMU measurement system and with its characterisation in the new facility at PTB, with an extended uncertainty of the order of 0.1%. Reaching the objective was possible with the collaboration of all the partners involved: POLITO and CIRCE, who provided the preliminary waveforms measured in the field, useful for the design of the measurement system and calibration facility, with the contribution of RISE which provided the necessary preliminary calibrations and above all of INRIM and PTB who built the measurement and calibration systems, respectively. The PwMU provides the measurement of the electrical quantities to the IPT charging station and above all, the measurement of its efficiency. In this measurement, the criticality is given by the voltage and current ripple at the battery, which have double pulsation with respect to the system resonant frequency, being this latter typically between 20 kHz and 85 kHz. The development of the new facility at PTB made it possible to properly calibrate the PwMU especially for on-board measurements. The new facility at PTB will support the research and use of inductively coupled power transmission systems, the evaluation and further development of the various electrical components, as well as the evaluation of the measured values of the electromagnetic emissions in relation to the actual electrical power.

## 4.2 Objective 2: Methods to determine the efficiency of static IPT stations.

The MICEV consortium successfully developed methods to determine the efficiency of a static wireless power transfer system with a relative uncertainty of  $10^{-3}$  taking the relevant parameters, particularly airgap and misalignment between the coupled coils into account. A double strategy was used to achieve this goal. On the one hand, a methodology for uncertainty estimation based on the instrumentation used for the PwMU was developed. On the other hand, a model and a simulation tool were created for charging stations, suitable for predicting their behaviour, knowing some input parameters, such as the geometry, topology and type of station and components. The model is able to simulate the behavior of the charging station and its efficiency, as a function of the relevant parameters, particular airgap and misalignment. A simplified version of the model simulator can be downloaded at the project website (<https://www.micev.eu/simulator>).

### 4.2.1 Assessment of the Overall Efficiency in WPT Stations (WPTS) for Electric Vehicles

The whole activity described in this section 4.2.1 was carried out by INRIM, for what concerned uncertainty analysis, while CIRCE and POLITO made available their charging stations for measurements. RISE, NPL, together with INRIM, CIRCE and POLITO all contributed to the implementation of the in-field measurements. The on-site assessment of the efficiency of a charging station is not a trivial process and is a topic of discussion for professionals. The efficiency of WPTS is an important parameter for both the user and the WPTS operators. A clear method to account for the parameters which can affect the correct determination of efficiency, such as in particular the accuracy of the meters and the effect of temperature, was set up. Such a method was tuned in the MICEV framework, and aimed at clarifying that, despite distorted waveforms at the charging stations, it is possible to reach a good accuracy in a wide temperature span (expanded uncertainty  $<0.5\%$  between  $5\text{ }^{\circ}\text{C}$  and  $40\text{ }^{\circ}\text{C}$  and  $<0.1\%$  between  $18\text{ }^{\circ}\text{C}$  and  $28\text{ }^{\circ}\text{C}$ ). Analysis initiated from the measurement conditions and the actual waveforms recorded at two WPTS with differently rated power. The analysis highlighted the possibility of verifying class 0.5 meters on-site, desirable for this type of application.

The proposed method is clearly discussed in [4]. In the following a summary of the main steps is reported.

Power transfer efficiency is the ratio between two electrical power quantities measured at the same time instant: the power measured on-board at the batteries,  $P_{board}$  in the following, and the power adsorbed and measured at the electrical grid, which is commonly a three-phase power called  $P_{grid}$  in the following. The overall efficiency is defined as  $\mu = \frac{P_{board}}{P_{grid}}$ .

Starting from the above definitions, if the measurements of the two powers can be considered uncorrelated, as reasonably it is, the uncertainty on the measurement of the efficiency can be obtained through the formula

$$u_{\mu}^2 = \mu^2 \cdot \left[ \left( u_{rP_{grid}} \right)^2 + \left( u_{rP_{board}} \right)^2 \right] \quad (2)$$

where  $u_{\mu}$  is the measurement uncertainty on the overall efficiency,  $u_{rP_{grid}}$  is the measurement relative uncertainty on the measured power from the grid and  $u_{rP_{board}}$  is the measurement relative uncertainty on the measured power at the batteries.

#### Measurements on-board

A possible solution to assess the uncertainty is to carry out the determination, by means of a Fourier transform, of the frequency components of the voltages and currents in order to obtain the values. The overall power on-board will be:

$$P_{board}(U_0, I_0, U_1, I_1, \phi_1, U_2, I_2, \phi_2, \dots) = \sum_{k=0}^{NA} U_k \cdot I_k \cdot \cos \phi_k \quad (3)$$

where  $U_0$  and  $I_0$  are the DC voltage and current respectively,  $U_i$ ,  $I_i$  and  $\phi_i$  are the AC voltage, current and phase angle of the  $i^{\text{th}}$  harmonic respectively, and  $NA$  is the considered number of harmonics of the AC ripple. For the uncertainty calculation, we refer to equation (3) limiting the analysis to the DC component and the first harmonic of the AC component (ripple). As will be clearly seen in the following, this is not a significant limitation. In case of uncorrelated components. The related uncertainty on power results is:

$$u_p^2 = (u_{\Delta U_0}^2 \cdot I_0^2 + u_{\Delta I_0}^2 \cdot U_0^2) + (u_{\Delta U_1}^2 \cdot I_1^2 + u_{\Delta I_1}^2 \cdot U_1^2) \cdot \cos^2 \phi_1 + u_{\Delta \phi_1}^2 \cdot U_1^2 \cdot I_1^2 \sin^2 \phi_1 \quad (4)$$

being  $u_p$  the uncertainty on the measured power,  $u_{\Delta U_0}$  and  $u_{\Delta I_0}$  the measurement uncertainties on the DC voltage and DC current respectively, and  $u_{\Delta U_i}$ ,  $u_{\Delta I_i}$  and  $u_{\Delta \phi_i}$  the measurement uncertainties on the AC voltage, current and phase angle of the  $i^{\text{th}}$  harmonic, respectively.

The relative uncertainty on the measured power is consequently:  $u_{rP_{board}} = \frac{u_p}{P_{board}}$  (5)

The calculation must consider that a power analyser is normally used for power measurement and that a transducer (usually a coaxial shunt) is used for current measurement. The calculation of the uncertainty that develops from the formula (4) and (5) is summarised in Figure 5. It can be easily demonstrated that the distortion that appears in the current and voltage ripples at the batteries has a negligible effect on power.

### Measurements on the grid side

The calculation of the uncertainty is performed for all the phases. We name the three phases  $\rho$ ,  $\sigma$  and  $\tau$ . In the following, for simplicity, the first phase ( $\rho$ ) is considered extending the result to the other phases.

$$U_{\rho grid}(U_{\rho 1}, \phi_{u\rho 1}, U_{\rho 2}, \phi_{u\rho 2}, \dots) = U_{\rho 0} + \sum_{k=1}^n U_{\rho k} \cdot (\cos k\omega t + \phi_{u\rho k}) \quad (6)$$

$$I_{\rho grid}(I_{\rho 1}, \phi_{i\rho 1}, I_{\rho 2}, \phi_{i\rho 2}, \dots) = I_{\rho 0} + \sum_{k=1}^n I_{\rho k} \cdot (\cos k\omega t + \phi_{i\rho k}) \quad (7)$$

$$P_{\rho 1} = P_{\rho fund} = U_{\rho 1} \cdot I_{\rho 1} \cdot \cos(\Delta\phi_{\rho 1}) \quad (8)$$

The distortion power, for each phase, can be computed as the difference between the measured power and the first harmonic (or fundamental) power:

$$P_{\rho\_distortion} = P_{\rho\_meas} - P_{\rho\_fund} \tag{9}$$

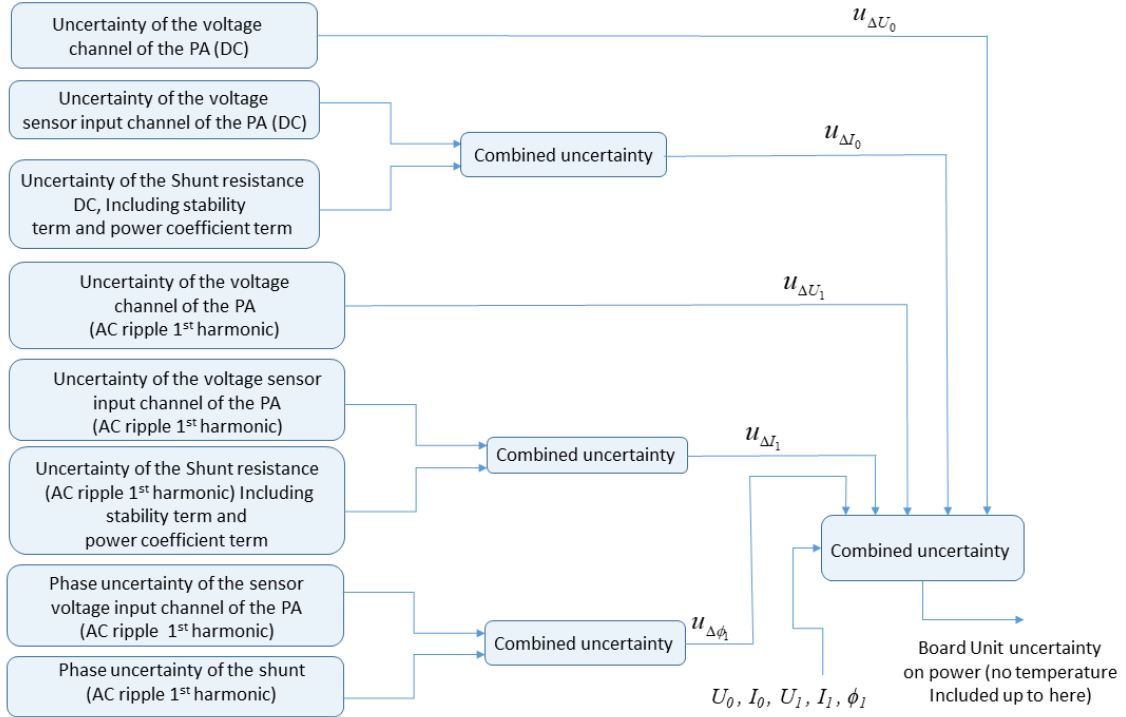


Fig. 5 Uncertainty computation process for the measurements on-board. PA means power analyser.

$$\Delta P_{distortion} = P_{\rho\_distortion} + P_{\sigma\_distortion} + P_{\tau\_distortion} \tag{10}$$

$$P_{fund} = P_{\rho\_fund} + P_{\sigma\_fund} + P_{\tau\_fund} \tag{11}$$

The uncertainty due to the harmonic distortion can be expressed as: 
$$u_{rP\_distortion} = \frac{|\Delta P_{distortion}|}{\sqrt{3} \cdot P_{fund}} \tag{12}$$

Taking all distorted power as uncertainty is to follow a conservative approach. Such an approach is a good practice when, as in the analysed cases, data on calibration beyond the power frequency are not available, which commonly happens in current calibrations at power frequency. According to formula (12) the computed values in ppm for  $u_{rP\_distortion}$  in two experimented WPTS were found below 225 ppm.

**Temperature effect**

Uncertainty calculation is preliminary done at room temperature, in a temperature range in which the calibration performances of the instruments used are guaranteed, usually between 22 ° C and 24 ° C. We call these extremes of temperature  $T_1$  e  $T_2$ . Concerning the grid measurements, the calibration uncertainty is considered valid in the temperature range  $T_1 \leq T \leq T_2$ . Therefore, the grid side temperature variation  $\Delta\theta$  is defined as follows:

$$\forall \theta^* < T_1 \quad \Delta\theta = T_1 - \theta^* \tag{13} \quad \text{and} \quad \forall \theta^* > T_2 \quad \Delta\theta = \theta^* - T_2 \tag{14}$$

The final standard relative uncertainty is then computed as:

$$u_{rP_{grid}} = \sqrt{\left(u_{rP_{grid}}\right)_{cal}^2 + \left(u_{P_{grid\_Temp}} \cdot \Delta\theta\right)^2 + \left(u_{rP_{grid\_distortion}}\right)^2} \tag{15}$$

The power analyser and the transducer for on-board measurements may have a slightly different calibration stability temperature range. We denote this range with  $T_1^* \leq T \leq T_2^*$ . We will therefore have:

$$\forall T^* < T_1^* \quad \Delta T = T_1^* - T^* \quad (16)$$

$$\forall T^* > T_2^* \quad \Delta T = T^* - T_2^* \quad (17)$$

The complete expression of the uncertainty related to the measurements on-board is then:

$$u_{rP_{board}}(T) = \sqrt{u_{rP_{board}}^2 + \left( \frac{\Delta u_{rP_{board}}(T)}{\Delta T} \cdot \Delta T \right)^2} \quad (18)$$

where  $u_{rP_{board}}$  is computed in (5).

The methodology summarised above was applied to the measurements performed at two charging stations with the PwMU. The results with the greatest measurement uncertainty, mainly due to a greater harmonic distortion of voltage and current, are shown in Table 3.

Table 3 - overall efficiency uncertainty vs temperature. WPTS worst case (SU = Standard Uncertainty.  $\mu = 0.89$ )

$T$ (°C)	$T$ (°C)	On-board SU $u_{rP_{board}}(T)$ (ppm)	Grid SU $u_{rP_{grid}}(T)$ (ppm)	Efficiency SU $u_{\mu}(T)$ (ppm)	Expanded Uncertainty $U_{\mu}(T)$ (‰)
6	40	1154	1879	1963	3.93
10	36	831	1417	1462	2.92
11	35	750	1302	1337	2.67
14	32	513	959	968	1.94
15	31	435	846	847	1.69
16	30	360	735	728	1.46
17	29	287	625	612	1.22
18	28	222	518	502	1.00
20	26	150	324	318	0.64
21	25	150	253	262	0.52
23	24	150	225	241	0.48

A second step of the study was the assessment of the measurement uncertainty of the instrumentation mounted at the WPTS: to this purpose the existing measurement system at the two WPTSs were analysed. Discrepancies on power measured on-board and on the power measured at the grid connection point, as well as the measured overall efficiency, were found lower than 0.5%. The observed results underline that the class 0.5 for the instrumentation at the WPTS can be suitable, as already envisaged by the standards for similar applications like railways.

#### 4.2.2 Modeling the efficiency of static wireless power transfer stations

When performing a measurement, the order of magnitude of the quantity to be measured is usually known. This allows the best setting of the instrumentation, the measuring ranges of the devices, the replacement of some transducers with others of a more suitable range. In a charging station, the power to be measured, as well as voltage and current, easily change by an order of magnitude. It is very useful to place alongside the measurement system a forecasting model which, by determining the behavior of the physical system, gives comfort about the correctness of the order of magnitude of the measured quantities. The physical model, therefore, in addition to avoiding trivial errors in the execution of the measurement, allows optimisation of the instrument.

#### Modeling and simulation tool

In this section, the developed low-complexity behavioral analytical models of the mutual inductance between the coupling coils of WPTSs, as functions of their reciprocal position, are briefly mentioned. These models are

extremely useful in the characterisation and design optimisation of WPTSs. A multi-objective genetic programming algorithm is adopted to generate models ensuring an optimal tradeoff between accuracy and complexity. The training and validation datasets needed for the generation of the models are obtained by performing numerical full 3-D electromagnetic simulations. The resulting behavioral models allow the accurate and fast evaluation of the WPTS coils mutual inductance, over a wide range of misalignment conditions, enabling easier system analysis and optimisation. The main work performed in order to develop these models has been done by UNISA and UNICAS, based on the modeling of POLITO (WPTS-1) and CIRCE (WPTS-2) WPT stations. POLITO and CIRCE provided all the technical input to UNISA and UNICAS, while AALTO developed an alternative approach for verification. The models developed are described in [5] and [6]. CNRS performed an assessment of the magnetic flux density variability using stochastic models, also in view of the assessment of the human exposure [7]-[8]. In the following a brief insight about behavioural models.

The coupling coil pairs analysed here are taken from the two real WPTSs mentioned above. The geometry for each system is shown in Figs. 6 and 7, highlighting the transmitting (Tx) and receiving (Rx) coils. The models also include an aluminum structure (which simulates the vehicle chassis) and some ferrite parts. These two systems differ in many aspects, including the architecture and the operating frequency. For instance, in WPTS-1, the Tx coil is longer than the Rx one, whereas for WPTS-2 the dual setup is adopted. Their main parameters are summarised in Table IV.

The WPTS-1 coil pair has been analysed by means of the full 3-D numerical solver, an electromagnetic code developed in-house by UNICAS solving magneto-quasi-static equations, based on integral formulation. This approach is well tailored for the problems analysed in the project, since it only requires meshing the conducting and magnetic regions, avoiding meshing air and imposing fictitious boundaries to close the problem. The results have been validated against measurements with satisfactory agreement. The WPTS-2 coil pair has been analysed by the same code and validated by comparison with a commercial 3D tool.

Table 3 - Parameters of the analysed WPTS coil pairs

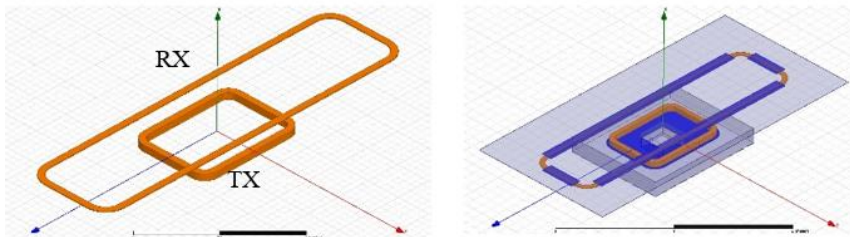


Fig. 6 - WPTS-2: the coil pair, and the complete pad, with aluminium (grey) and ferrite (blue)

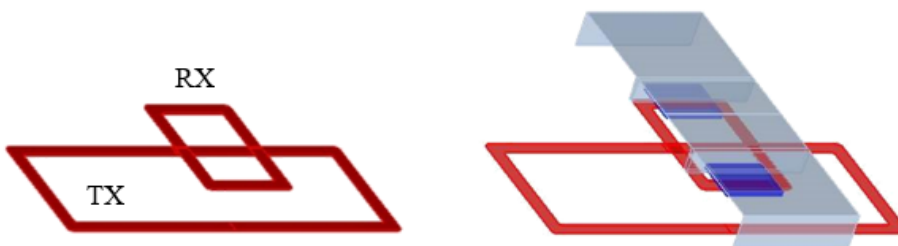


Fig. 7 - WPTS-1: the coil pair, and the complete pad, with aluminium (grey) and ferrite (blue)

Parameter	WPTS-1	WPTS-2
Frequency	85 kHz	25kHz
Tx wire cross-section	28 mm <sup>2</sup>	300 mm <sup>2</sup>

Parameter	WPTS-1	WPTS-2
Rx wire cross-section	28 mm <sup>2</sup>	50 mm <sup>2</sup>
Tx number of turns	10	2
Rx number of turns	10	4
Tx inner dimensions	1.5m x 0.5m	0.653m x 0.864m
Rx inner dimensions	0.3m x 0.5m	2.640m x 0.750m
Vertical distance between coils	20 cm	15 cm
Shield conductivity	33.4 MS/m	38 MS/m
Ferrite relative permeability	2000	2000

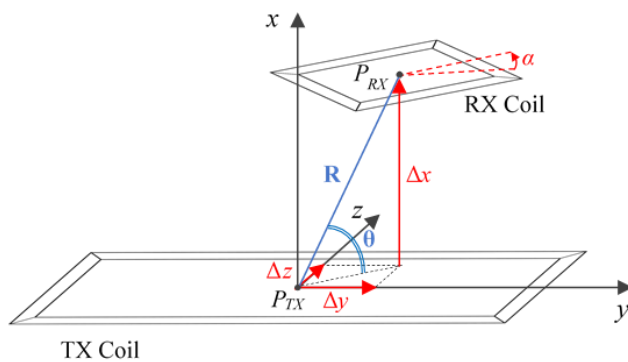


Fig. 8 - WPTS coils: their reciprocal position is given by the coordinates  $\{\Delta x, \Delta y, \Delta z\}$  of the Rx coil center point  $P_{RX}$  with respect to the Tx coil center point  $P_{TX}$  (located in the origin), and  $\alpha$  by rotation angle

The coils of the two WPTSs were studied in a generic position, characterised by a vertical distance,  $\Delta x$ , and by a misalignment in the horizontal plane ( $y, z$ ), described by a displacement ( $\Delta y, \Delta z$ ) and a rotation  $\alpha$  (see Fig. 8). The First Harmonic Approximation (FHA) analytical model of the two WPTSs has been first adopted to perform the sensitivity analysis. Mutual inductance information deriving from models developed by UNICAS has been incorporated in the UNISA FHA simulations.

The cost of a simulation, based on the 3D numerical code, may easily become unaffordable when a large number of case-studies are to be mapped as a function of the geometrical parameters, as in a sensitivity analysis. To overcome this problem, a behavioral model of mutual inductance  $M$  has been derived by using the Genetic Programming algorithm. In this

approach, the population is composed of models and their evolution is dictated by classical genetic operations, such as selection, cross-over, mutation. This approach has been here applied to model the dependence of  $M$  on  $\Delta x, \Delta z$ , and  $\alpha$ . Specifically,  $M_{behav}(\Delta x, \Delta z, \mathbf{p}(\alpha))$  is given as a function of  $\Delta x$  and  $\Delta z$ :

$$M_{behav} = -p_0 \Delta z^{1.5} \exp(-p_1 \Delta x) + p_2 \exp(-p_3 \Delta x) \tag{19}$$

and is parametrised with respect to  $\alpha$ , being  $\mathbf{p}(\alpha)$  a vector of model coefficients dependent on  $\alpha$ :

$$p_i = a_{i,0} \cos(2\alpha) + a_{i,1}, \quad i = 0,1,2,3 \tag{20}$$

Figure 9 shows the percent error introduced by the behavioral model in the 300 test conditions of the training data set (300 different values of coils misalignment in terms of  $\Delta x, \Delta z$  and  $\alpha$ ) for WPTS-1.

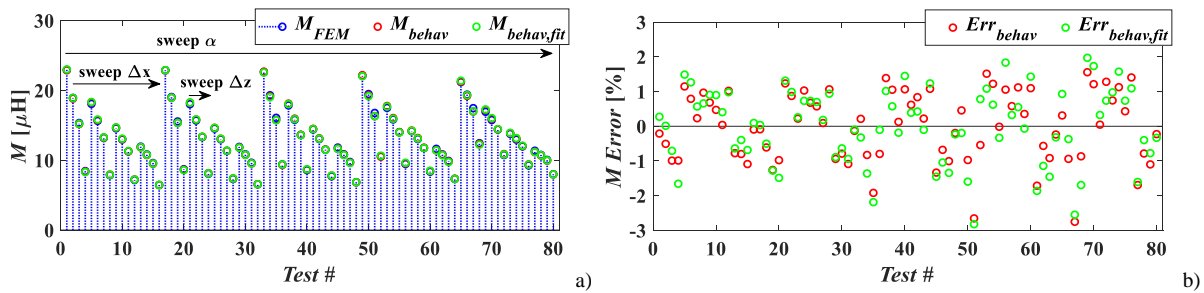


Fig. 10 - Predictions of behavioral modl for WPTS-1: (a) mutual inductance values obtained by FEM simulations (blue markers), by model with the original  $p_i$  coefficients (red markers) and by model with the cosine approximations of  $p_i$  (green markers); (b) relative percent errors.

The behavioural model is an excellent compromise between the accuracy of the FEM calculation and the need to develop an analysis in a short time. More details in [5] and [6].

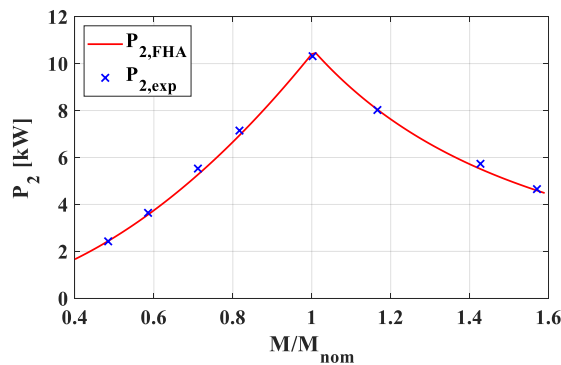


Fig. 9 - . FHA model predictions (solid lines) and experimental data (cross markers) for mutual inductance sweep (note that  $M_{nom}=14.3\mu\text{H}$ ).

#### 4.2.3 Comparing computed and measured results, benchmarking, and conclusions

The FHA model of WPTS-1 was validated by means of measurements performed by INRIM and POLITO, which resulted to be in good agreement.

The parameters that were varied for the comparison between measurements and calculations is the coils mutual inductance  $M$ . Fig. 10 shows the FHA model predictions (solid lines) and experimental data (cross markers) for mutual inductance sweep (note that  $M_{nom}=14.3\mu\text{H}$ ). The results are shown in terms of power at the batteries.

The quantities that have been measured for comparison are as follows: i) voltage at the

batteries  $V_{2dc}$ , ii) current at the batteries  $I_{2dc}$ , iii) power at the batteries  $P_2$ .

#### Benchmarking

To the MICEV consortium knowledge, there are no specific regulations for inductive charging stations that specify the accuracy of the power measurement for the installed instrumentation. For this reason, the investigation on the accuracy of the installed measurement systems at two charging stations (benchmarking) was carried out. Benchmarking was designed and carried out by TUV SUD PS, CIRCE, INRIM and POLITO. Measurements were performed at two different power levels. The expected result of the comparison, confirmed by the measurements, are in accordance with the few regulations in force (such as e.g. ANSI C12.20, or EN 50463-2 for railway transport) and show relative discrepancies not exceeding 0.5%.

#### Conclusions

In conclusion, the objective of the project has been achieved; the efficiency of a static wireless power transfer system with a relative uncertainty of  $10^{-3}$  can be determined. A method to assess the uncertainty was provided by this project study.

- The target of a relative expanded measurement uncertainty  $10^{-3}$  can be obtained also during in-field measurements both on the efficiency measurements as well as on the power measurements in a limited range of temperature. With the considered instrumentation utilised in the PwMU, the temperature range is  $18^\circ\text{C} \leq T \leq 28^\circ\text{C}$ . This may require mild air conditioning of the rooms where the instrumentation is located.
- In a system with many parameters with high variability as in a charging station, it is possible to envisage the measured power and efficiency. So, is it possible to associate to the measurement system a numerical

forecasting model that foresees the results of the measurement as a function of misalignment and vertical displacement.

- The model has been validated by comparison with the measurements on a charging station. Measurements and computations are in agreement with maximum discrepancies on the measured power lower than 15%. The study also highlighted that it is desirable to install class 0.5 instruments for power / energy measurement and that it is possible to verify them on site.

### 4.3 Objective 3: Dynamic inductive power transfer

Dynamic WPT was analysed through a wide modelling survey and experimental measurements. A modelling approach was developed by UNICAS, UNISA and POLITO, based on the POLITO charge while driving (CWD) system, developed during the European projects eCo-FEV (Efficient Cooperative infrastructure for Fully Electric Vehicles) and Fabric (Feasibility analysis and development of on-road charging solutions for future electric vehicles). Moreover, a laboratory facility equipped with a moving carriage, including a receiving coil, was utilised to perform electric and efficiency measurements. The main results are summarised below. More details and results can be found in [9]

#### 4.3.1 Modeling Dynamic wireless power transfer and identification of relevant parameters

##### System description

The system under study to investigate the behaviour of dynamic inductive power transfer consists of a series of 50 transmitters 1.5 m long and 50 cm large with an inter-space of 50 cm. Each transmitter is supplied by a dedicated DC/AC H-bridge converter. The POLITO CWD system included the installation of the electrical equipment in an existing full-electric light commercial vehicle, without modifications to the vehicle chassis. A rated power of 20 kW was chosen for each single DC/AC converter of the IPT system. This power level is sufficient to match the power consumption of the adopted vehicle up to about 70 km/h in condition of perfect lateral alignment with the transmitter. In the following sections the system is discussed in more details.

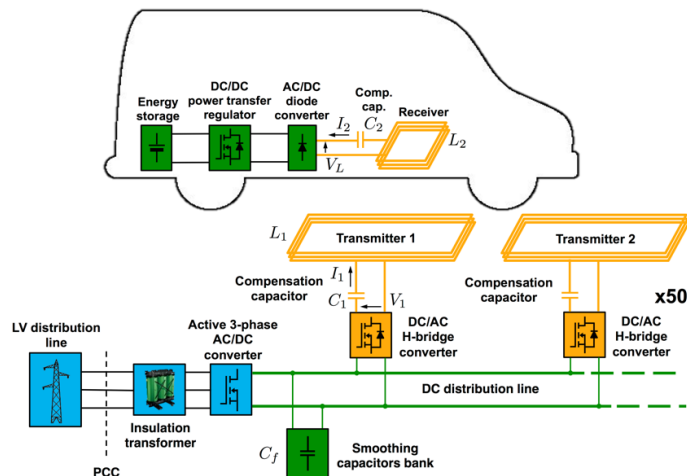


Fig. 11 - Electrical infrastructure for the dynamic IPT proposed by the team of the Politecnico di Torino

##### Sub-system modeling

The modelling phase required dedicated tools for different sub-systems. The magnetic coil pair was studied using an integral code, accounting for the small penetration depth of the eddy currents and for the open-boundary nature of the structure under study. In particular, the electrical parameters of the transmitting and receiving coils were extracted and compared with the values measured in the laboratory prototype, showing a good agreement with a maximum error on the inductance evaluation of 3.7%.

A theoretical study about the effect of motion of the receiving structure above the transmitting coil was performed, in order to investigate the dynamic effects on the mutual inductance. It was found that the dynamic

effects on the electric and magnetic parameters are negligible for realistic geometries (transmitter lengths) and in a wide range of speeds, as shown in Figure 12.

From the analysis of the electric and magnetic parameters, a behavioural model of the mutual inductance was developed, allowing the prediction of the mutual inductance for any possible trajectory of the receiving coil. This allowed to reproduce fast and reliable results for different driving trajectories without the requirement of complex simulations.

An accurate uncertainty estimate of the mutual inductance value against the longitudinal displacement  $\Delta y$  and the lateral misalignment  $\Delta z$  was achieved. The relevant sensitivity (Sobol) indices are  $S_{\Delta y}=0.684$  and  $S_{\Delta z}=0.349$ , which means the mutual inductance is highly dependent on both geometrical parameters when considering variation along both axes at the same time such as a normal trajectory for a car along a road.

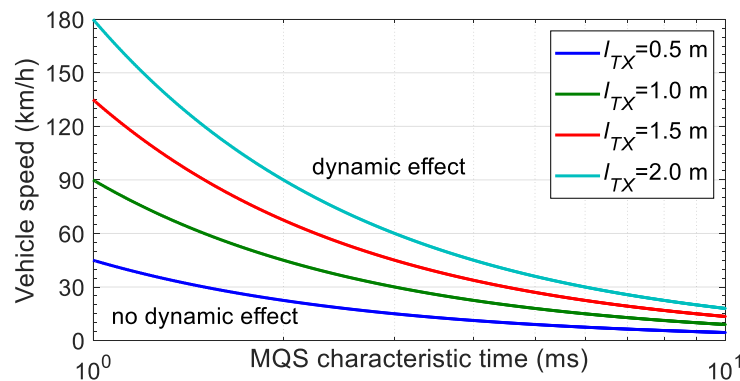


Fig. 12 - Dynamic WPT system: maximum vehicle speed as a function of the electromagnetic characteristic, time parametrised to the Tx coil length: for a given length, the corresponding curve is the boundary between the regions where the dynamic effects are/are not negligible

However even if the Sobol index for the direction of motion is bigger than the Sobol index for the lateral misalignment, the latter cannot be totally neglected within the control loop.

An analysis of the literature dealing with dynamic inductive charging was performed during the MICEV project by TU-Delft and POLITO. The analysis showed that it is difficult, if not impossible, to reproduce the systems and results proposed by different authors. Papers systematically lack key data and technological information for an extensive quantitative comparative analysis. For this reason, a specific tool for dynamic inductive power transfer based on the previous models was used to study the effect of different traffic conditions and car misalignments. In particular, two quantities were analysed at the three-phase, 50 Hz section of the charging station:

- the first is the total harmonic distortion of the current and voltage signals, defined as

$$THD = \frac{\sqrt{\sum_{k \neq f} X_k}}{X_f}$$

where  $X_f$  is the fundamental harmonic at 50 Hz, and  $X_k$  is the  $k$ th harmonic.

- The second quantity is related to the reconstruction relative root mean square error, normalised with respect to the magnitude of the fundamental harmonic  $X_f$ , obtained with  $N$  harmonics of the Fourier series:

$$\varepsilon_x(N) = \frac{1}{X_f} \sqrt{\frac{1}{kT} \int_c^{c+kT} \left[ x(t) - \sum_{n=-N}^N c_n e^{j \frac{2\pi n t}{T}} \right]^2 dt}$$

where the internal integral is extended over an integer multiple  $k$  of the period of the signal (voltage or current). For each waveform is calculated the maximum frequency necessary to reconstruct the signal with rms error lower than  $10^{-3}$

The reference case was a straight trajectory, i.e.  $z_0 = 0 \text{ m}$  and  $\alpha_0 = 0^\circ$ , with a vehicle speed of  $v_0 = 50 \text{ km/h}$ . The vehicle passed above the first coil of the series. The resulting voltage and current waveforms are reported in **Error! Reference source not found.**

The harmonic analysis showed that the THD of the voltage is lower than 6%, whereas for the current can be as large as 121%.

**Error! Reference source not found.** reports the reconstruction error versus the harmonic range used for the reconstruction of the original signal with the Fourier series. Neglecting the ripple due to converters, it can be seen that the harmonic contribution to the voltage is negligible up to about 30 kHz, where the error starts decreasing, crossing the target of  $10^{-3}$  at around 49 kHz. On the contrary, the current has a significant harmonic content also at low frequencies, however the target relative error of  $10^{-3}$  is met at around 38 kHz.

In order to explore the effect of multiple parameters (number of vehicles, delay among the beginning of the charging phase for each vehicle, speed of vehicles, and trajectory), about 3000 different random combinations were studied. The statistical analysis of the results, showed that:

- The voltage has a low *THD* (maximum value of 11.4 %) with respect to the current (maximum value 258.6%)
- The maximum bandwidth necessary to reconstruct the original signal with a relative error of  $10^{-3}$  is 75.6 kHz for the voltage, whereas the current requires at most 51.5 kHz.

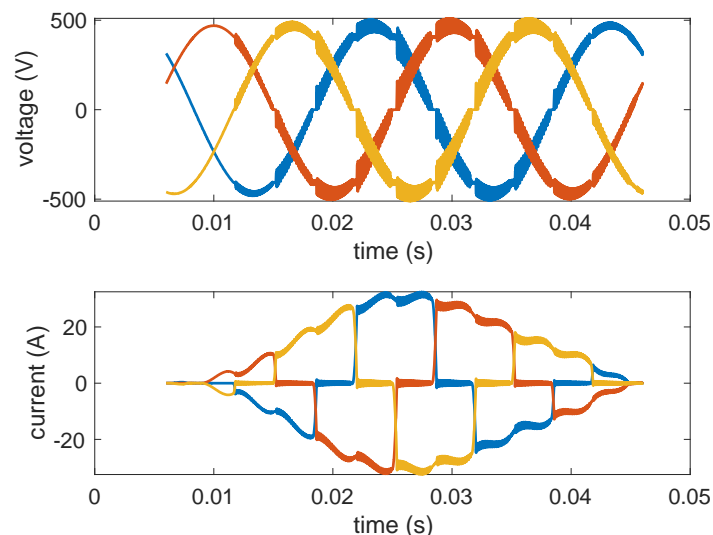


*Fig. 13 - Voltage and current waveforms of the reference case*

4.3.2 A measurement system special requirements

The PwMU developed for static IPT was used by INRIM and POLITO to perform some measurements on the laboratory test rig, where the receiver was positioned on a carriage and manually moved at low speed. Measurements have been performed at the battery side, transmitting and receiving coils, and grid connection point.

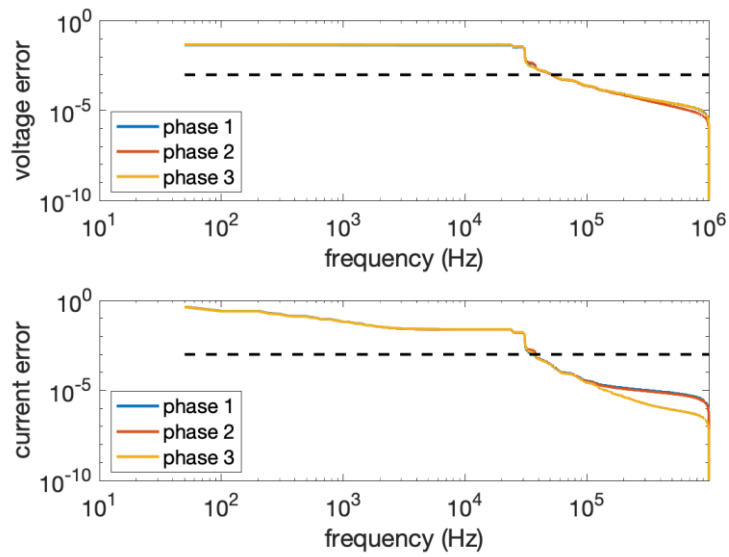


Fig. 14 - Reconstruction error increasing the number of harmonics in the Fourier series.

In the experiments, the carriage is pushed by hand by two operators and the push occurs with an initial cue and the carriage swings. Likewise, the carriage is stopped by two thrust stops, which again determine an oscillation upon arrival. The initial and final mechanical oscillations affect the measured voltage and electric current. The trend of the current to the receiving coil, measured at the facility, is shown in Figure 15. The receiving and transmitting coils start with a slight overlapping at the edges, and therefore the initial voltage and current to the receiving coil are not zero. When the carriage starts, once the initial oscillation is exceeded, the electric current in the receiving coil increases as the overlapping increases and therefore also the coupling of the coils rises. The overall modulation visible shows local oscillations. The acquisition of the entire transient signal is very demanding in terms of sampling interval, sampling frequency and, above all, necessary memory.

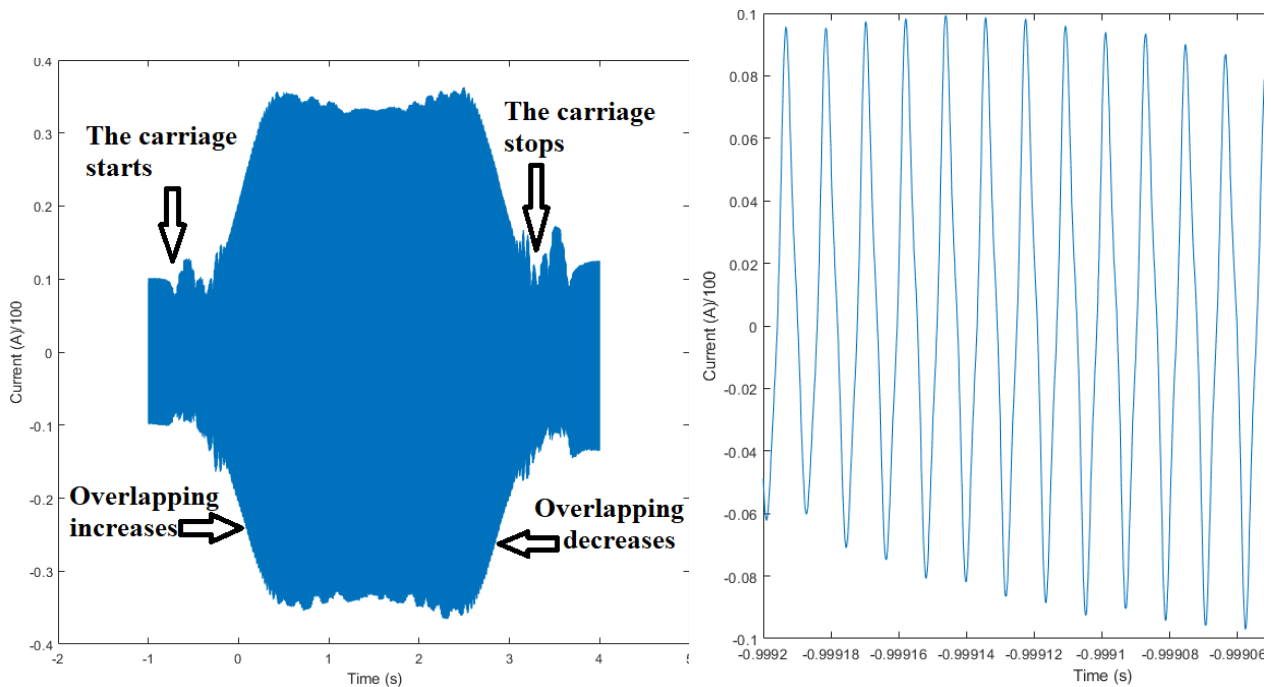


Fig. 15 - Electrical current measured at the receiving coil. Left: all the transient. Right: local zoom.

For the measurements on board (receiving coil, batteries), it was necessary to use a tool other than the PwMU. A measurement system was therefore adapted to perform dynamic measurements, based on a digital storage oscilloscope with large memory and large frequency bandwidth (e.g. Tektronix MSO or Lecroy MDA). Figure 16 shows the voltage and current at the DC load (batteries) and the voltage and current at the Tx coil.

In a more complex case, when the vehicle moves over a charging lane made of several transmitting coils and with an electric motor connected to the battery, the measurement becomes more challenging.

- When the vehicle proceeds for a significant distance on a series of coils of the same station at constant speed, for a time that is a multiple of the sampling time, it is possible to consider measuring the power transferred and the power absorbed by determining the efficiency, which will be a function of speed. This however involves acquiring the entire transient of the passage on at least two coils. Considering a coil length of 1.5 m, a speed range between 5 km/h and 100 km/h, and a distance between the coils of 10 m, this means to consider acquisitions that have a duration from about 360 ms up to 7.2 s. The acquisition cards chosen for the PwMU do not have enough memory for such long acquisitions at 5 MS/s while the power analysers have difficulty in accurately measuring non-periodic and/or poorly repeatable signals. The only possibility that seems reasonable is to record waveforms with multi-channel recording systems with very high memory and sampling capacity.

- If the speed is not constant, it will be necessary to rely on energy measurements. An algorithm that evaluates and counts the occurrence of the transient (passage on the coil) will be associated with the power measurement algorithm. Consequently, the calculation of power and energy takes place after a certain number of passages on the coils and, at the end of the journey or at the request of the driver, the energy calculation at the current instant is presented.

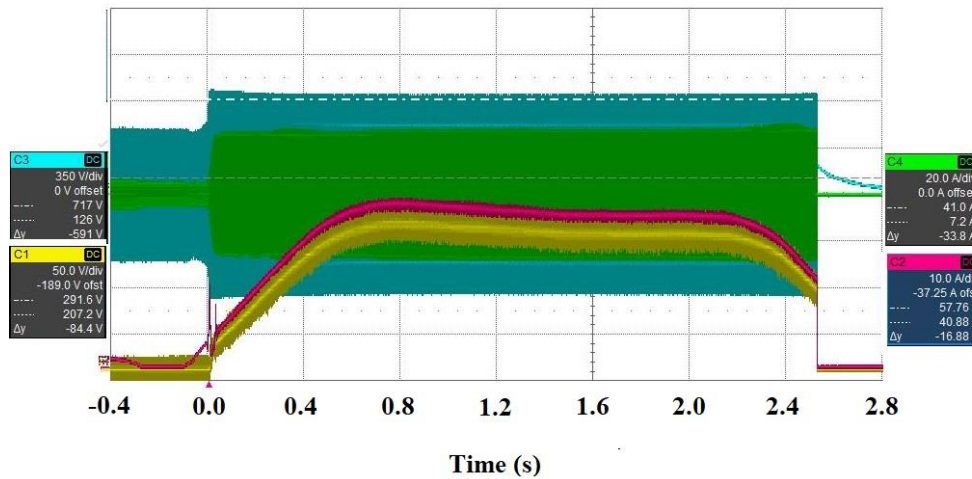


Fig. 16 - Voltage (yellow) and current (red) at the DC load (batteries). Voltage (blue) and current (green) at the transmitting coil. Average speed 7 km/h..

### 4.3.3 Additional considerations and conclusions

#### Foreign object detection

TU-Delft and INRIM analysed the effect of foreign objects on the efficiency and harmonic distortion. Such an effect was studied through an experimental approach and through simulations. A downscaled measurement setup was adopted, with an output power of 2 kW. An aluminium can, a metal key and a bolt were used as foreign objects. The result of the measurement is reported in Table 5. The efficiency changed of about 1% in presence of aluminium cans, with lower effects for smaller objects. The total harmonic distortion was not affected by foreign objects. Similar results were obtained through the simulation of the system. As a conclusion, metallic objects could be hardly detected measuring the variation of electrical parameters. In fact, the power losses associated to common objects (can, ring, nail) were negligible with respect to the rated power of the IPT system. For this reason, different technologies, such as image recognition or ultrasonic sensors must be used for the purpose.

Table 5 - Measured results with foreign objects

Case	Condition	Power Loss Increase (W)	Efficiency Decrease (%)	Temperature Rise ( $T_{amb}=19^{\circ}\text{C}$ ) ( $^{\circ}\text{C}$ )	THD of Transmitter Current (%)	THD of receiver Current (%)
1	Coke can, centred	30.3	1.159	20	0.6761	1.0513
2	Coke can, shifted	1.4	0.049	7	0.6391	0.8933
3	Key, point A	2.3	0.104	14	0.6627	0.8955
4	Bolt, point A	2.2	0.088	13	0.6326	0.8374

#### Multi-objective optimisation of the DIPT system

A 20 kW DIPT system was optimised using a multi-objective optimisation algorithm developed by TU-Delft, with the cooperation of POLITO, UNISA and UNICAS. The objectives included gravimetric/area power density, aligned efficiency and misaligned efficiency. Considering that the receiver should be compatible with the transmitter from both static IPT and dynamic IPT systems, the analysis was divided into static and dynamic

optimisation. By analysing the Pareto front of the static multi-objective optimisation, the aligned efficiency is 96.66%. In dynamic optimisation, the receiver geometry is fixed based on the results of the static optimisation. The optimal efficiency in the dynamic case was higher than 94.69% within the studied range of misalignment. Finally, the winding current THD of the DIPT system using series-series and double-sided LCC compensations were investigated through circuit simulations. It was found that the winding current THD of the series-series compensated system can reach 2.54%, while that of the LCC compensated system is lower than 0.277%.

## Conclusions

The study on dynamic IPT systems was carried out by six partners of the MICEV project using both computations and measurements when available. From the analysis the objective of the study has been achieved. In particular we can draw the following conclusions:

- A computational tool for dynamic inductive power transfer was used to study the effect of different traffic conditions and car misalignments. A thorough analysis of the dynamic of the coil pair showed that the dynamic effects on the electric and magnetic parameters (resistances, self and mutual inductances) are negligible for realistic geometries of the sub-systems and in a wide range of vehicle speeds.
- For the same reason stated above, losses and efficiencies do not change significantly from the static to dynamic charging on a wide range of speeds.
- An accurate uncertainty analysis of the mutual inductance value against the longitudinal displacement  $\Delta y$  and the lateral misalignment  $\Delta z$  was computed. The relevant Sobol indices are  $S_{\Delta y}=0.684$  and  $S_{\Delta z}=0.349$ , means that the mutual inductance is highly dependent on both parameters when considering variation along both axis at the same time such as a normal trajectory for a car along a road. However even if the Sobol index for the direction of motion is bigger than the Sobol index for the lateral misalignment, the latter cannot be totally neglected within the control loop.
- Using a multi-objective optimisation of the complete system it is possible to obtain an IPT system with 96.7% of efficiency in static and 94.7% in dynamic conditions.
- The measurements performed on the laboratory test rig showed that the PwMU had limits for dynamic measurements, due to the limits of the measurement software and above all, of the memory of the acquisition cards, given the long transient to be acquired with a high sampling rate (at least 5 MS/s). The requirements for a measurement system for measurements in a dynamic IPT charging station have been clarified.
- The study of foreign object detection proved that objects could be hardly detected measuring the variation of electrical parameters. In fact, the power losses associated to common objects (can, ring, nail) were negligible with respect to the rated power of the IPT system. For this reason, different technologies, such as image recognition or ultrasonic sensors must be used for the purpose.
- The analysis of the THD pointed out that, basically, the required bandwidth for measurements does not change with respect to the static measurements but the memory required by the system changes.
- As a final remark, the analysis of the literature in this field showed that it is difficult, if not impossible, to reproduce the systems and results proposed by different authors. Papers systematically lack key data and technological information for an extensive quantitative comparative analysis.

#### 4.4 Objective 4: Human exposure to magnetic fields

##### 4.4.1 The new calibration facility at NPL and its validation.

Various National Metrology Institutes (NMIs) and some calibration laboratories have the capability to characterise AC magnetic field meters. To characterise AC magnetic field meters and to achieve the lowest uncertainties, a number of basic requirements need to be satisfied:

- An environment with minimal AC magnetic field background;
- A stable field generating source, such as Helmholtz coils with good temperature stability and minimal long-term drift;
- A field generating source of sufficient size such that field uniformity does not impact the measurement uncertainty;
- Other equipment used, such as current shunts to measure current, should be characterised at the frequencies of interest.

NPL has several Helmholtz coil systems that allow uniform magnetic fields to be generated at their centre that are used to assess and characterise various types of magnetic sensor including the AC magnetic field meters of the type used in the MICEV project for the measurement of AC magnetic fields in and around WPT systems.

Helmholtz coils are used to generate a uniform region of magnetic field along the axis of the coil. When the separation,  $s$ , of two identical coils is equal to the radius,  $r$ , the Helmholtz condition is satisfied. A typical setup is shown in Figure 17 where  $s$  is the separation between coil 1 and coil 2,  $r$  is the coil radius and  $a$  is the distance from each coil to the mid-plane,  $a = s/2$ .

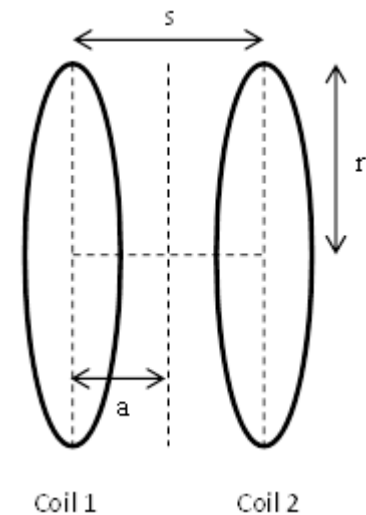


Fig. 17 - Diagram of the arrangement of Helmholtz coil

Helmholtz coil systems are calibrated to determine their coil constant, the magnetic field strength to current ratio. The Helmholtz coil systems are calibrated at DC using a proton resonance magnetometer to obtain the lowest uncertainties and at AC using a single turn search coil.

The coil constant of an ideal Helmholtz coil system, in A/m/A, is given by the relationship:

$$\frac{H}{I} = \frac{8}{5\sqrt{5}} \frac{N}{r} \quad (x)$$

where  $H$  is the axial magnetic field strength, in units of ampere per meter, A/m,  $I$  is the current in the coils, in units of ampere, A,  $N$  is the number of turns on each coil,  $r$  is the radius of each coil, in units of meters, m.

For the DC coil constant determination, the traceability to the SI is obtained via frequency for the magnetic field measurement and to DC resistance (calibrated standard resistor) and DC voltage (calibrated digital voltmeter (DVM)) for the current measurement. For the AC determination, the change in coil constant with increasing frequency (or frequency dependence) is assessed using a single turn search coil. The single turn search coil has no significant frequency dependency over the frequency range considered here, and the change in coil constant is determined with respect to the DC value. AC traceability to the SI is obtained via AC/DC transfer standards for AC resistance (calibrated shunts) and AC voltage (calibrated DVM). All measurements are traceable to National Standards held and maintained at NPL.

Along with the determination of the coil constant, other factors including the uniform field region at the centre of the coils, temperature stability and long-term drift are also assessed and contributions included in the associated measurement uncertainties that support NPL's United Kingdom Accreditation Service (UKAS) ISO/IEC 17025 accreditation for these measurements.

##### 4.4.1.1 New Helmholtz Coil System

The requirements of a new Helmholtz coil system, developed during the MICEV project are: frequency range: 10 kHz to 150 kHz; Field range: up to 100  $\mu$ T; Target expanded uncertainty: 5%.

Based on initial designs, including field uniformity modelling, the prototype coils were 3D printed and wound using Litz wire. To meet the target expanded uncertainty, a field non-uniformity (variation) of less than 2% is required at the centre of the coils where the magnetic field probes are positioned. From the modelling, to obtain a field non-uniformity of between 1% and 2%, the radius of the coils was determined to be 188 mm and 141 mm respectively. To accommodate a calibration of a magnetic field instrument with 100 cm<sup>2</sup> external probe of the type used within the project for on-site WPT testing, a coil radius of 150 mm was selected. To obtain an ideal Helmholtz configuration the separation between the coils is also 150 mm. To reduce the change in coil constant with increasing frequency, as few a number of turns as possible is preferred to limit impedance effects such as inter-winding capacitance which would limit the maximum field the coils can generate. Based on the physical dimensions and number of turns (4 per coil), the design coil constant was 24 μT/A, therefore the Litz wire current rating should be at least 5 A to allow 100 μT to be generated.

The fabricated coils are shown in Figure 18.



Fig. 18 – The new Helmholtz coil with Narda ELT-400 magnetic field instrument with 100 cm<sup>2</sup> external probe.

As part of the coil’s characterisation, the DC and AC coil constants were determined. The change in coil constant is less than 0.2% at 150 kHz. Shown in Figure 19 (left) is a plot of the change in coil constant and (right) a comparison in radial uniformity between the design and measured values.

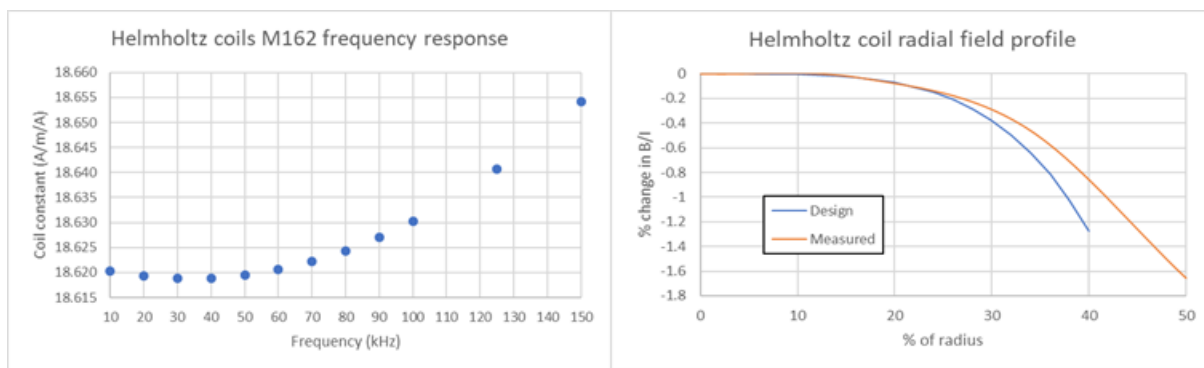


Fig. 19 – Plot of frequency response (left) and radial field profile (right).

Shown in Figure 20 is a comparison of the maximum fields generated between the existing high frequency coils (labelled M139 in blue) used for the characterisation of AC magnetic field meters and the new coil (in orange). The new coils allow a much larger AC field to be generated compared to the existing systems.

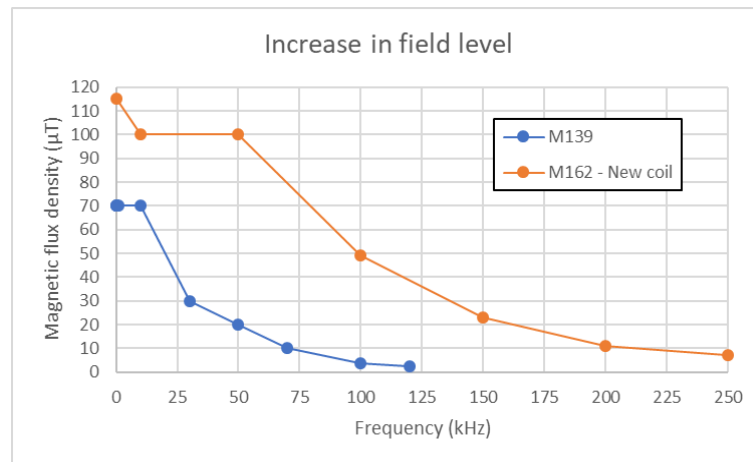


Fig. 20 – Comparison of field and frequency levels generated in existing and new HF coils.

#### 4.4.1.2 Calibration of the New Helmholtz Coil System and intercomparison

As part of the calibration of the coil system, a measurement uncertainty for the determination of the coil constant was assessed, and all relevant contributions were accounted for. The uncertainty includes contributions for the field measurement (magnetometer) and current measurement (resistor/DVM), and also includes:

- i) Alignment of magnetometer – to confirm maximum field is being measured,
- ii) Uniformity of field – determined for the sensor calibrated during the measurement,
- iii) Change in background magnetic field during the measurement - in this case the calibration is performed in an ambient field cancelation system,
- iv) Repeatability,
- v) Drift, long term stability – difference from calibration-to-calibration.

Depending upon the item under calibration, this leads to a calibration uncertainty for AC magnetic field instruments of 0.5% ( $k=2$ , 95% confidence level) at 1 kHz to 0.9% ( $k=2$ , 95% confidence level) at 150 kHz.

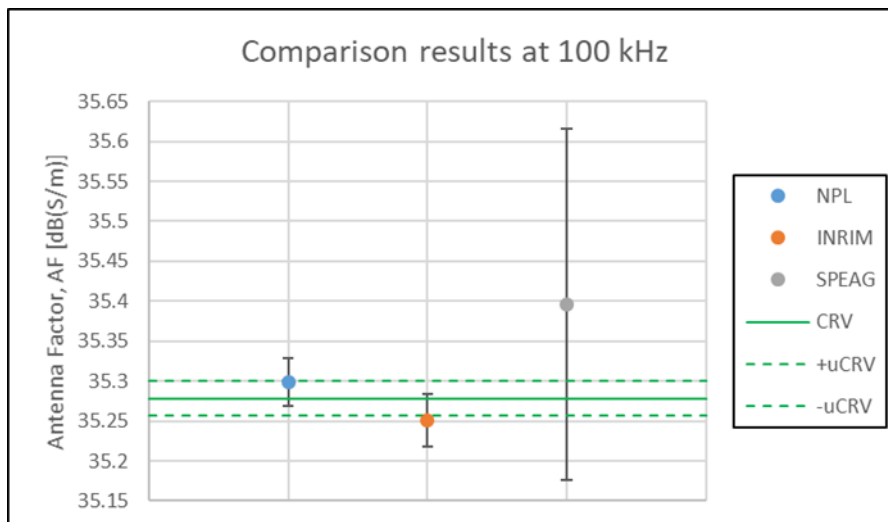


Fig. 21 – Comparison of field and frequency levels generated in existing and new HF coils.

These uncertainties were reported by NPL during the inter-comparison including INRIM and SPEAG to validate their measurements systems over the frequency range 10 kHz to 100 kHz. The comparison results at 100 kHz can be seen in Figure 21.

During the initial evaluation of the new Helmholtz coil system, field generation was extended to a frequency of 250 kHz but with a much-reduced field produced at the centre of the coils, approximately 7.25  $\mu$ T. Further evaluation at this frequency is required before the calibration of AC instruments can be routinely conducted.

The full specification of the new coil system is given in Table 6.

Table 6 – AC magnetic field specification of new coil.

	Coil system	Project	
	M162	requirement	met
Frequency range	DC to 150 kHz Operational up to 250 kHz	10 kHz to 150 kHz	✓
Maximum field capability	DC to 50 kHz: 100 $\mu$ T 50 kHz < f $\leq$ 100 kHz: 50 $\mu$ T 100 kHz < f $\leq$ 150 kHz: 23 $\mu$ T 150 kHz < f $\leq$ 250 kHz: 7.25 $\mu$ T	100 $\mu$ T <u>Comparison:</u> 10 kHz to 30 kHz: 100 $\mu$ T 40 kHz to 100 kHz: 25 $\mu$ T	✓ ✓ ✓
Expanded uncertainty (k=2)	0.5 % at 1 kHz 1.0 % at 150 kHz	5.0 % up to 150 kHz	✓

Besides the new calibration facility developed at NPL, SPEAG has also setup a calibration system and a new meter for MF gradient measurements up to 100  $\mu$ T/m and developed a novel method and procedure for evaluating compliance of sources with strong gradient MF such as wireless power transfer systems [11].

#### 4.4.2 To develop measurement protocols for the assessment of the human exposure

Measurement protocols for the assessment of the human exposure to the electromagnetic fields generated by IPT system for electric vehicles have been developed, taking the compliance with the limits indicated by the guidelines of the International Commission on Nonionizing Radiation Protection (ICNIRP) into account.

The development of the measurement protocols was based both, on the experience in-field (measurements), gained at the two charging stations of CIRCE and POLITO made available for the project, and through appropriate calculation models used either for the sensitivity analysis of the results to physical parameters and for dosimetric assessment.

The consortium preliminary validated its computational codes on a realistic IPT benchmark problem, and then the two charging stations were modeled by partners. The physical properties of the car body were analysed and the critical scenarios were studied both the light and heavy vehicles. Exposure scenarios were defined for vehicle occupants and bystanders. SPEAG generated the advanced bioelectromagnetic models of adults, children, and infants of the Virtual Population (ViP), also modifying the postures according to a simulation protocol agreed. Dosimetric analysis were performed based on a developed database of the B-field components.

CNRS performed a sensitivity analysis of the results in terms of magnetic field distribution around and inside the vehicle on the variation of a car body physical properties while SPEAG developed a similar analysis in terms of induced electric field on the variation of dielectric and conductive properties of the tissues. The stochastic models based on Kriging and Polynomial chaos expansions resulted to provide a fast approach to estimate uncertainty contributions and variabilities of different parameters, both physical and geometrical were applied to models of a IPT charging station. Specifically, the combination of Kriging and Polynomial chaos expansion provides a very good predictor. The analysis of a realistic and complex situation, including a light vehicle, showed that for a given set of parameters, relying on 50 % of the total number of sample data points is accurate enough to build a correct sensitivity analysis relevant to the level of exposure. Also, it was assessed that the influence of the relative permeability and the coil misalignment along the axis of motion is clearly negligible against the misalignment along the other axes and the car-body conductivity [10].

A novel method and procedure for evaluating compliance of sources with strong gradient magnetic fields such as wireless power transfer systems were developed by SPEAG and presented in [11], while preliminary distributions of magnetic flux densities inside and around a vehicle were presented in [12].

An example of a complete study concerning a dosimetric analysis using measurements and calculations, which also includes the uncertainty assessment of magnetic field measurements, was developed by SPEAG, INRIM, NPL, RISE and CIRCE in [13], while SPEAG developed a specific analysis regarding the safety evaluations of electrically short implants in human beings [14].

Numerical aspects related to the accuracy and the computational efficiency of numerical dosimetric simulations are widely discussed in [15] by INRIM, SPEAG and POLITO, where two alternative numerical methods for dosimetric analysis, respectively based on electric vector potential and electric scalar potential formulations, are compared for the electric field computation in highly detailed anatomical human models. The analysis has highlighted a different behaviour of the two alternative finite element formulations, depending on the characteristics of the voxelised anatomical human model and spatial distribution of the magnetic field.

NPL, INRIM, RISE, POLITO, CIRCE and CNRS, with the help of SPEAG, collected the experience gained during the project in the electromagnetic metrology and human exposure problems related to inductive charging of electric vehicles, both from a modelling and experimental point of view, in the "Best Practice Guide for the assessment of EMF exposure from vehicle Wireless Power Transfer systems" [16]. The document (BPG in the following) is open access and distributed in the project website (<https://www.micev.eu/>).

The BPG are designed for people who approach the assessment of human exposure in vehicles and around inductive charging stations. BPG are intended to complement the published standards in use and those currently being developed by international technical organisations and bodies. Figure 22 shows the BPG cover.

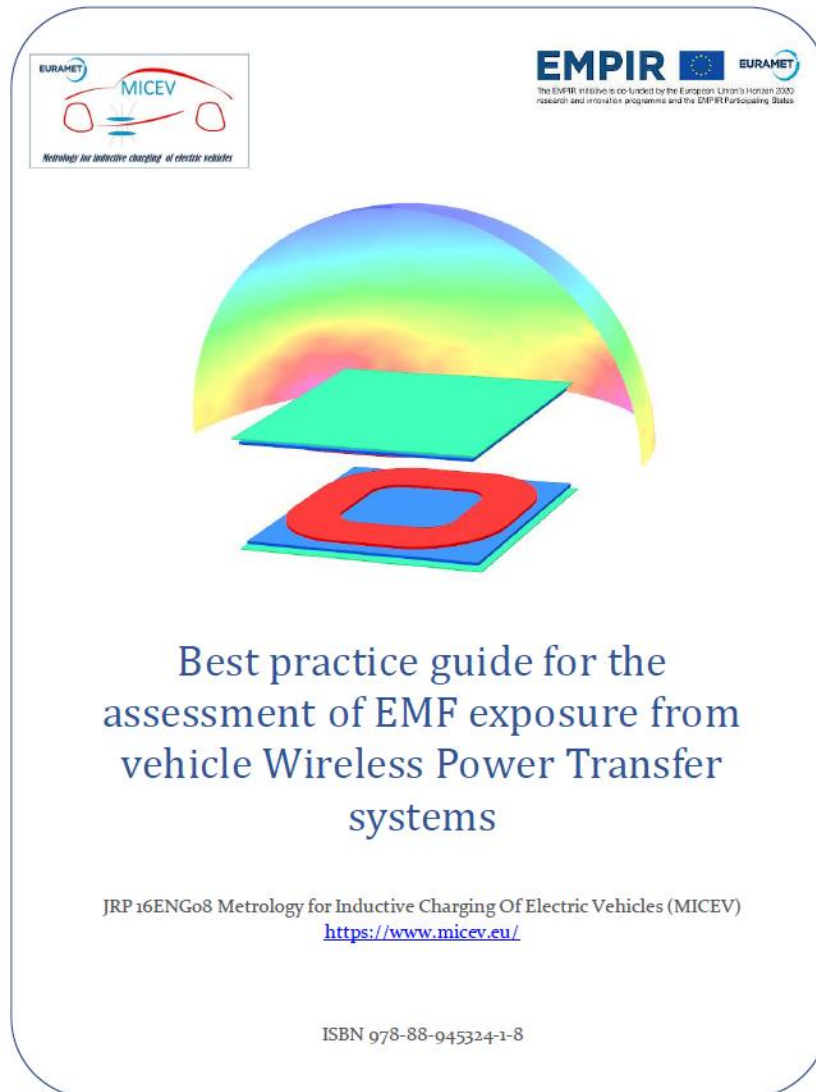


Fig. 22 – BPG cover.

BPG seeks to assemble the experience gained by MICEV consortium in the field of human exposure assessment and to provide information for the assessment of exposure through experimental measurements and validated calculations. The calculation of the induced quantities, in particular the induced electric field and electric currents in the tissues, is of fundamental importance for the determination of human exposure. From the point of view of dosimetry, for obvious reasons of feasibility, the calculation replaces the measurement. Therefore, a whole chapter of the BPG covers the choice of instruments and the description of the correct settings for both the magnetic field calculations and the dosimetric calculations.

The document particularly focuses on the following challenges:

- the testing framework, including the common layout of charging stations;
- means and methods to perform:
  - o measurements of the magnetic flux density in and around a vehicle;
  - o measurements of limb currents;
- means and methods to perform:

- o analytical calculation of magnetic flux density levels for EMF exposure assessment;
- o computation of the induced electric fields in human beings.

The guidelines contain some appendices, which include the following: a real example of a charging station; some tables with the exposure limits referred to in the BPG; a brief comparison between existing standards; a test case of a numerical code to calculate the sources [17]; some results on the sensitivity of simulated exposure metrics to the variations in tissue properties and, finally, the measurement capabilities of European national metrological institutes concerning AC magnetic fields at the frequency range of interest for Wireless Power Transfer systems (WPTs).

Objective 4 was fully achieved.

## 5 Impact

The project hosted a training course on “Wireless Charging of Vehicles - Measurements, modelling, and human exposure,” in November 2019 at PTB, Germany. The training course also presented the project’s preliminary results to a total of 20 external participants, which included four people from other NMI’s, 8 people from other universities, five people from companies including instrument manufacturers and engineering companies and the remaining were students.

A website for the project was created at [www.micev.eu](http://www.micev.eu) and a blog hosted in the project website was populated. The project has been disseminated via a number of different press releases, media interviews and TV and radio clips including ANSA (Italian national press agency), TG Leonardo (Scientific news on Italian National broadcasting RAI3) and Smart City: Materials, Technology and People- at Materials Village - Material ConneXion hub Italia during "Milano Design Week". In addition, the project has published 15 open access publications, a publicly available “Best Practice Guide” and a dataset, and given 28 conference presentations, such as Conference on Precision Electromagnetic Measurements (CPEM 2018 and 2020), IEEE Conference on Electromagnetic Field Computation (CEFC 2018 and 2020), 2019 AEIT International Conference of Electrical and Electronic Technologies for Automotive (AEIT Automotive) and International Symposium on electromagnetic fields (ISEF 2019), International Conference on Synthesis, Modelling, Analysis and Simulation Methods and Applications to Circuit Design (SMACD 2018 and 2019), IEEE International Conference on Electronics, Circuits and Systems (ICECS 2020), IEEE International Symposium on Circuits and Systems (ISCAS 2020) and MICEV Final Workshop.

The final virtual workshop of the project was organised on a double live channel, on the Zoom and YouTube platforms. The event aroused good interest with over 100 registered participants, 90 actual participants in the live session with a stable average of 65 persons in each instant of the workshop. The workshop remained available on YouTube for deferred viewing, where it has a total (as of March 2021) of over 250 views.

### *Impact on industrial and other user communities*

An advisory Stakeholder Committee has been established for the project consisting of thirteen stakeholders including instrument manufacturers, automotive engineering companies, a local transport company, an electric company and some SME’s. The Stakeholder Committee interacts with the project website via the project website and meetings. A car company (Volvo) is also participating in the project as collaborator.

The project has developed new measurement capabilities of direct relevance to accredited laboratories, manufacturers of MF meters and manufacturers of electric current, voltage, and power meters. Manufacturers of EVs and their component suppliers, manufacturers of forklift and automatic vehicles in the industrial environment will also benefit from the project’s results.

In particular, the project developed a new voltage standard a step-up calibration procedure at INRIM for the voltage transducers used in IPT systems, that can take into account the actual waveforms registered in related applications. Moreover, the project developed a new calibration facility at PTB for calibration of power analysers, suitable for the measurement of power at the frequency levels required by these applications (ripple up to 150 kHz, uncertainty of the reference power standard of the order of  $10^{-3}$  relative). The new measurement capabilities related to the facility will be accessible to companies and laboratories, especially manufacturers of electric current, voltage and power meters and electric companies interested in IPT.

A system for traceable calibration of MF meters was realised at NPL. This facility is suitable for MF up to 100  $\mu$ T (for 10 kHz–150 kHz, with both sinusoidal and non-sinusoidal waveforms) and is available to accredited laboratories and manufacturers of MF meters. Another facility for MF field gradients calibration (gradiometers) has also been developed at SPEAG.

The project produced specific theoretical investigations and measurements on power losses in the IPT chain. Future payment systems in public charging systems and stations will take advantage from this research data by helping to clarify what the consumer pays for, i.e. the transmitted or received energy.

### *Impact on the metrology and scientific communities*

The project has developed a measurement system for the calibration of voltage dividers up to 200 kHz at INRIM. This was realised by a step-up procedure using an amplitude and phase precision comparator. The latter is based on high resolution and high-speed digitisers, equipped with software programs in Labview™ for

the simultaneous determination of the voltages on the two channels and their phase differences. The original step-up calibration procedure, together with a new reference voltage resistive capacitive divider for voltages up to 1 kV and bandwidth up to 200 kHz developed during this project, are intended to extend traceability of voltages above 100 V up to (and beyond) 200 kHz [2]. This new measurement system was utilised to calibrate the voltage transducers of the PwMU.

A new phantom power standard was realised at PTB. The facility can be applied for DC currents affected by harmonics determining AC power up to 150 kHz. New CMCs were submitted by PTB to Euramet for AC power measurements in the frequency range between 15 Hz and 150 kHz, for active power, reactive power, and apparent power. The target uncertainty in the range of  $10^{-3}$  was met. The new CMCs based on the new PTB standard, will support the research and the use of inductively coupled power transmission systems, the evaluation and further development of the various electrical components, as well as the evaluation of the measured values of the electromagnetic emissions in relation to the actual electrical power. Other metrology institutes will be able to expand their measurement capability in this power and frequency range by tracing them to this standard.

NPL, developed a new calibration facility for measuring the MF, which has extended the measuring range of magnetic induction in Europe, for the low frequency, from 20  $\mu$ T at 100 kHz up to 100  $\mu$ T at 150 kHz. The new facility was validated by conducting a successful inter-comparison between three project partners. A measuring system for the MF gradient has been developed at SPEAG in the same frequency range.

#### *Impact on relevant standards*

The consortium disseminated the guide [16] to EURAMET Technical Committee Electricity and Magnetism (TC-EM), Sub Committee Power and Energy. The EURAMET TC-EM chair disseminated the guide to all the national TC-EM contacts. At least two positive feedbacks were received by the consortium.

IEA is the International Energy Agency. IEA IA-HEV Task 26 aimed to develop a greater global understanding of wireless power transfer systems and interoperability through a focused study of WPT technologies being developed in the participating countries. IEA Task 26 was contacted by CIRCE, but Task 26 completed its job before the end of MICEV project. However, the chair of the task provided anyway interesting feedback to the work of the consortium with particular reference to BPG.

IEC CISPR D WG1 committee was contacted by RISE and the chair and secretary found the BPG interesting, so they have circulated it to their expert working group members.

SPEAG represented the consortium in the IEC TC 106 committee. In particular, SPEAG operated IEC TC 106 WG9 "Addressing methods for the assessment of WPT related to human exposures to electric, magnetic and electromagnetic fields", and with the group drafting new standard PT63184 "Human exposure to electric and magnetic fields from wireless power transfer systems". SPEAG provided input in the discussion about new normative document PT63184. WP9 of IEC 106 added a new methodology based on gradient measurements to reduce the exposure overestimation. SPEAG was very active in developing this method and has also developed corresponding instrumentations as part of the MICEV project. SPEAG provided input to the committee working group and presented the BPG to the chair of the IEC TC106 WG on PT63184.

CEI TC 106 is the Italian committee mirror of IEC TC 106, which provided an important feedback and will consider the BPG for the preparation of one part of new Italian national guidelines concerning human exposure to WPT systems. Moreover, CEI TC 106 included INRIM in the Working Group on WPT for the preparation of a first technical report on this subject, preliminary to guidelines.

#### *Longer-term economic, social and environmental impacts*

The EU is committed to reducing greenhouse gas emissions by 2050 to a level which is 80–95 % below 1990 levels. In the 2050 Energy Roadmap a key goal amongst others will include "no more conventionally-fuelled cars in cities". Actions aimed at increasing the use of electric transport will directly contribute to these objectives and hence this project is centred on EU political strategies concerning transport.

According to "Research and Markets" report 2020 on "Global Electric Vehicle Charging Stations Market Report 2020: 2018-2019 Value and Volume, 2020 Estimates and Forecast to 2027", edited by Meticulous Market Research Pvt. Ltd., the electric vehicle charging stations market is expected to grow at a CAGR of 39.8% from 2020 to 2027 to reach \$29.7 billion by 2027; whereas, in terms of volume, the market is expected to grow at a CAGR of 31.8% from 2020 to 2027 to reach 15,025.5 thousand units by 2027.

Based on the charging station type, plug-in charging stations segment is estimated to account for the largest share of the overall electric vehicle charging stations market in 2020. The growth in this segment is mainly

driven by the government and automakers initiatives to expand the level 3 plug-in charging station infrastructure. However, the wireless charging stations market is expected to witness rapid growth during the forecast period. The rapid growth of this segment is primarily attributed to the automaker's initiatives for the development of wireless charging stations technology and government funding for the installation of the wireless charging stations.

In the future, payment systems will be widely spread in inductive public charging systems and stations. Therefore, it must be clear exactly what the consumer pays for, in terms of the transmitted or received energy. This project will facilitate the implementation of wireless charging for EVs on public roads and highways, thus providing public assurance on the safety and the cost of using EV vehicles and inductive charging technologies.

## 6 List of publications

- [1.] M. Zucca, P. Squillari and U. Pogliano, "A Measurement System for the Characterization of Wireless Charging Stations for Electric Vehicles," in *IEEE Transactions on Instrumentation and Measurement*, vol. 70, pp. 1-10, 2021, Art no. 9001710, doi: 10.1109/TIM.2020.3046908, [Link](#)
- [2.] M. Zucca, U. Pogliano, M. Modarres, D. Giordano, G. Crotti, D. Serazio, "A Voltage Calibration Chain for Meters Used in Measurements of EV Inductive Power Charging", 2018 Conference on Precision Electromagnetic Measurements (CPEM 2018), Paris, 2018, DOI: 10.1109/CPEM.2018.8500831 ([Link](#))
- [3.] M. Zucca ; M. Modarres ; U. Pogliano ; D. Serazio, "1 kV Wideband Voltage Transducer, a Novel Method for Calibration and a Voltage Measurement Chain," *IEEE Transactions on Instrumentation and Measurement*, vol. 69, no. 4, pp. 1753-1764, April 2020, doi: 10.1109/TIM.2019.2912589. [Link](#)
- [4.] M. Zucca, V. Cirimele, J. Bruna, D. Signorino, E. Laporta, J. Colussi, Miguel A. A. Tejedor, F. Fissore, U. Pogliano, "Assessment of the Overall Efficiency in WPT Stations for Electric Vehicles" *Sustainability* 13, no. 5: 2436, 2021. [Link](#)
- [5.] K. Stoyka, R. A. Pessinatti Ohashi, N. Femia, "Behavioral Switching Loss Modeling of Inverter Modules", Proc. 15th International Conference on Synthesis, Modeling, Analysis and Simulation Methods and Applications to Circuit Design (SMACD), 4 pages, Prague, Czech Republic, 2-5 July 2018, DOI 10.1109/SMACD.2018.8434850, [Link](#)
- [6.] G. Di Capua, N. Femia, K. Stoyka, G. Di Mambro, A. Maffucci, S. Ventre. "Mutual Inductance Behavioral Modeling for Wireless Power Transfer System Coils," in *IEEE Transactions on Industrial Electronics*, vol. 68, no. 3, pp. 2196-2206, March 2021, doi: 10.1109/TIE.2019.2962432., [Link](#)
- [7.] S. Deshmukh, P. Lagouanelle, and L. Pichon, "Assessment of human exposure in case of wireless power transfer for automotive applications using stochastic models", *ACES Journal*, Vol. 35, No. 3, March 2020, [Link](#)
- [8.] Y. Pei, L. Pichon, M. Bensetti and Y. Le-Bihan, "Uncertainty quantification in the design of wireless power transfer systems", *Open Physics*, 18 (1), 2020, [Link](#)
- [9.] G. Di Capua, A. Maffucci, K. Stoyka, G. Di Mambro, S. Ventre, V. Cirimele, F. Freschi, F. Villone, N. Femia, Nicola, "Analysis of Dynamic Wireless Power Transfer Systems Based on Behavioral Modeling of Mutual Inductance" *Sustainability* 13, no. 5: 2556, 2021, [Link](#)
- [10.] P. Lagouanelle, O. Bottauscio, L. Pichon and M. Zucca, "Impact of parameters variability on the level of human exposure due to inductive power transfer," in *IEEE Transactions on Magnetics*, early access, doi: 10.1109/TMAG.2021.3062702, [Link](#)
- [11.] I. Liorni, T. Lisewski, M. H. Capstick, S. Kuehn, E. Neufeld and N. Kuster, "Novel Method and Procedure for Evaluating Compliance of Sources With Strong Gradient Magnetic Fields Such as Wireless Power Transfer Systems," in *IEEE Transactions on Electromagnetic Compatibility*, vol. 62, no. 4, pp. 1323-1332, Aug. 2020, doi: 10.1109/TEMC.2019.2924519, [Link](#)
- [12.] M. Zucca et al., "Metrology for Inductive Charging of Electric Vehicles (MICEV)," Proc. 2019 International Conf. of Electrical and Electronic Technologies for Automotive (AEIT AUTOMOTIVE), 4 pages, DOI: 10.23919/EETA.2019.8804498, [Link](#)

- [13.] I. Liorni, O. Bottauscio, R. Guilizzoni, P. Ankarson, J. Bruna, A. Fallahi, S. Harmon, M. Zucca, "Assessment of Exposure to Electric Vehicle Inductive Power Transfer Systems: Experimental Measurements and Numerical Dosimetry", *Sustainability* 2020, 12, 4573. [Link](#)
- [14.] I. Liorni, E. Neufeld, S. Kühn, M. Murbach, E. Zastrow, W. Kainz and N. Kuster., "Novel mechanistic model and computational approximation for electromagnetic safety evaluations of electrically short implants", *Physics in Medicine & Biology*, Phys. 225015 (14pp), Nov 2018, [Link](#).
- [15.] A. Arduino, O. Bottauscio, M. Chiampi, L. Giaccone, I. Liorni, N. Kuster, L. Zilberti, M. Zucca, "Accuracy Assessment of Numerical Dosimetry for the Evaluation of Human Exposure to Electric Vehicle Inductive Charging Systems", *IEEE Transactions on Electromagnetic Compatibility*, vol. 62, no. 5, pp. 1939-1950, Oct. 2020, [Link](#)
- [16.] 16ENG08 EMPIR MICEV consortium, "Best practice guide for the assessment of EMF exposure from vehicle Wireless Power Transfer systems", 2021, Edited by R. Guilizzoni, S. Harmon, M. Zucca, ISBN: 978-88-945324-1-8, available online at: <https://www.micev.eu/>
- [17.] M. Zucca, F. Freschi, I. Liorni, A. Fallahi, P. Ankarson, "Testing 3D modelling software. Modelling charging pads for WPT of electric vehicles for EM emissions simulation" (Version 1.0) [Data set]. 2021, Zenodo. [Link](#)

This list is also available here: <https://www.euramet.org/repository/research-publications-repository-link/>